AD-A066 176 NAVAL RESEARCH LAB WASHINGTON D C F/G 17/6
A FEASIBILITY STUDY OF THE USE OF SQUIDS FOR SCALAR FIELD MAGNE--ETC(U)
JAN 79 J H CLAASSEN

UNCLASSIFIED NRL-MR-3903 SBIE-AD-E000 268 NL

1 OF 1
ADA
066176

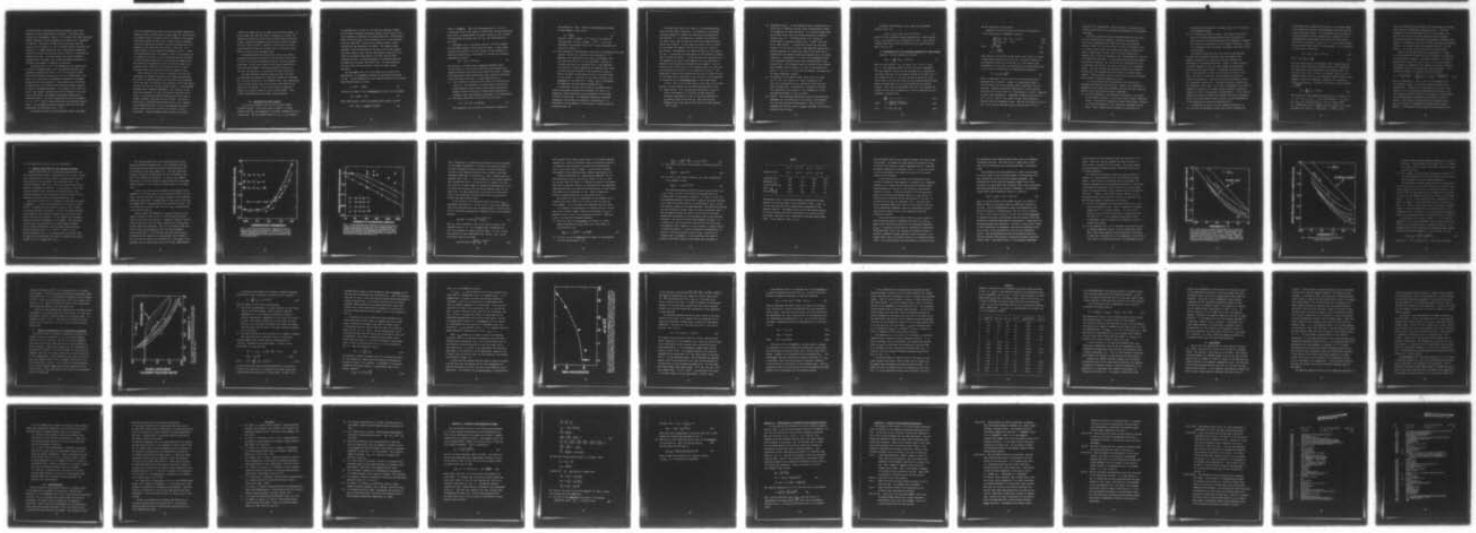

END
DATE
FILMED
5-79
DDC

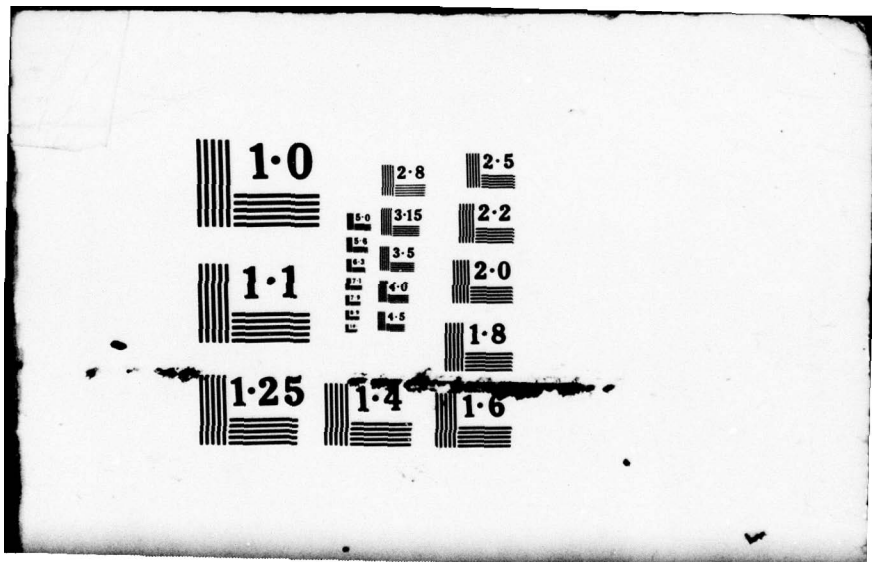
1·0
1·1
1·25
1·4
1·6
1·8
2·0
2·2
2·5
2·8
3·15
3·5
4·0
4·5
5·0

12
LEVEL III
DDC FILE COPY
AD A0 66176
DDC
RECEIVED
MAR 22 1979
B

SECURITY CLASSIFICATION OF THIS PAGE (When Data Entered)

REPORT DOCUMENTATION PAGE

READ INSTRUCTIONS BEFORE COMPLETING FORM

1. REPORT NUMBER: (14) NRL-MR-
NRL MEMORANDUM REPORT 3903

2. GOVT ACCESSION NO.

3. RECIPIENT'S CATALOG NUMBER

4. TITLE (and Subtitle)
(6) A FEASIBILITY STUDY OF THE USE OF SQUIDS FOR SCALAR FIELD MAGNETOMETRY.

5. TYPE OF REPORT & PERIOD COVERED
(9) Interim report on a continuing NRL problem

6. PERFORMING ORG. REPORT NUMBER

7. AUTHOR(s)
(10) J. H. Claassen

8. CONTRACT OR GRANT NUMBER(s)
APL Letter Agreement No. 600656, dated March 29, 1977.

9. PERFORMING ORGANIZATION NAME AND ADDRESS
Naval Research Laboratory
Washington, D. C. 20375

10. PROGRAM ELEMENT, PROJECT, TASK AREA & WORK UNIT NUMBERS
Work Unit P05-08.601

11. CONTROLLING OFFICE NAME AND ADDRESS
Applied Physics Laboratory
Johns Hopkins University
Laurel, Maryland 20810
(11) 7

12. REPORT DATE
January 1979

13. NUMBER OF PAGES
67

14. MONITORING AGENCY NAME & ADDRESS (if different from Controlling Office)
(12) 68p.

15. SECURITY CLASS. (of this report)
UNCLASSIFIED

15a. DECLASSIFICATION/DOWNGRADING SCHEDULE

16. DISTRIBUTION STATEMENT (of this Report)

Approved for public release; distribution unlimited.

(18) SBIE

DDC RECEIVED MAR 22 1979 B

17. DISTRIBUTION STATEMENT (of the abstract entered in Block 20, if different from Report)
(19) AD-E000 268

18. SUPPLEMENTARY NOTES
Prepared for the Applied Physics Laboratory, The Johns Hopkins University, under APL Letter Agreement No. 600656. This represents a progress report on the subject matter.

19. KEY WORDS (Continue on reverse side if necessary and identify by block number)
Scalar magnetometer
SQUIDS
Superconductive device
Magnetic anomaly detection (MAD)
Extremely low frequencies (ELF)

20. ABSTRACT (Continue on reverse side if necessary and identify by block number)
A single SQUID mounted on a platform subject to random motions in the earth's field will have large spurious components in its output. In order to recover the information of interest (changes in magnitude of the total magnetic field), it is necessary to combine the outputs of three mutually orthogonal sensors in an appropriate way. The coefficients characterizing this combination depend on the initial orientation of the platform relative to the earth's field, and thus must be determined dynamically. Several algorithms which deduce these coefficients from

(Continues)

DD FORM 1 JAN 73 1473 EDITION OF 1 NOV 65 IS OBSOLETE
S/N 0102-014-6601

SECURITY CLASSIFICATION OF THIS PAGE (When Data Entered)

251950

/B

20. Abstract (Continued)

a sequence of SQUID output data have been studied. In general the noise in the ambient field and/or the sensor noise (input noise) results in errors in the computed coefficients; these errors in turn lead to an additional source of noise in the processed output (processing noise). Computer simulations have been used to study interactions relating the frequency spectrum of the processing noise to the spectra of the input noise and platform oscillations. A number of practical considerations involved in a realization of a mobile platform system have also been analyzed. These include (1) the possibility of achieving a digitized output from the SQUIDS with sufficient linearity, dynamic range, and slew rate; and (2) the maximum deviations of the sensors from perfect orthogonality and gain uniformity that can be tolerated for given magnitude of platform oscillations.

TABLE OF CONTENTS

Section		Page
	List of Figures	ii
	List of Tables	iii
I	Introduction and Summary	1.
II	SQUID and Platform Requirements	6.
III	Processing the SQUID Outputs	9.
IV	Determination of the Processing Parameters by Least Squares	15.
V.	Computer Simulation of Least Squares Processing	21.
VI.	Adaptive Determination of Processing Parameters	35.
VII.	Conclusions	46.
VIII.	Recommendations	49.

LIST OF FIGURES

Figure		Page
1.	Dependence of the processing noise on the linearization parameter x, using least squares processing	23
2.	Dependence of the processing noise on number of samples per calibration interval, using residual processing	24
3.	The power spectral density of the processing noise as a function of frequency, assuming random-walk statistics for the external noise and using cumulative processing	32
4.	Same as Fig. 3, except using a longer calibration interval	33
5.	Same as Fig. 3, except assuming the external noise is Lorentzian	36
6.	Dependence of the acquisition time for adaptive processing on the feedback constant	40

LIST OF TABLES

Table		Page
I	Contribution of various errors to overall processing noise, for residual processing	28
II.	Summary of simulated results using the adaptive processing algorithm	44

I. INTRODUCTION AND SUMMARY

There is considerable interest in whether the high intrinsic sensitivity of SQUID devices ($\sim 10^{-5}\gamma/\sqrt{Hz}$) can be exploited in mobile applications, where the instrument is towed either underwater (as in the ELF receiver application) or in the air (MAD). The presently available instrument for such use, the optically pumped He vapor magnetometer, is a scalar device and has a noise level of $\sim 10^{-3}\ \gamma/\sqrt{Hz}$. A bit of thought will convince one that only scalar information about the magnetic field $\underline{H}$ is available under these circumstances. This is because a change in direction of $\underline{H}$ is indistinguishable, as far as the instrument is concerned, from a random rotation of the platform on which it is mounted. At the sensitivity levels quoted above, only changes in $|H|$ would be of interest.

A SQUID is intrinsically a vector component sensor, and thus will produce an output when it is rotated in a dc magnetic field unless it happens to be oriented exactly parallel to the field. Even if this were possible, the angular excursions would have to be less than $\sim 10^{-5}$ rad to avoid spurious signals comparable to the instrument sensitivity (assuming that the dc field is the earth's field, $\sim 5\times 10^{4}\ \gamma$). Thus the only practicable way to make use of SQUID's is to somehow combine the outputs of 3 sensors, aligned to be mutually orthogonal, in such a way that changes in the total field are recovered. Processing schemes to accomplish this have been given the acronym TRISCON (TRIaxial-

Note: Manuscript submitted November 9, 1978.

Scalar CONversion). The work reported here is an extension of previous analytical and experimental work at NRL [1-6] and later analytical work at APL [7,8].

In Sec. II we discuss the requirements on SQUID specifications that are set by the statistics of the platform oscillations. It is concluded that the maximum SQUID slewing rate is the most important limiting factor. Currently available SQUID systems should be adequate in an underwater towed buoy, but second-generation systems will probably be required on an airborne platform, unless significant reductions in the oscillations of the latter can be achieved.

In Sec. III we review the method by which three SQUID outputs can be combined to generate a scalar output. A number of parameters must be known to perform this computation. These include the effective offsets in the SQUID readings and the deviations of the sensors from perfect orthogonality. We show that the importance of the latter terms is governed by the magnitude of the platform excursions, and find that in a towed buoy they can safely be neglected. This considerably reduces the complexity of the computations required.

The remaining parameters used to process the SQUID data are different each time the system is used, since they depend on the orientation of the platform relative to the earth's field (as well as its magnitude) at the instant that the system is turned on. Hence, these parameters must be determined dynamically, and we have assumed that the only data available

is that from the SQUID sensors. The bulk of the work reported here involves evaluation and optimization of algorithms which use a sequence of SQUID data to determine the system parameters. To provide an appropriate figure of merit, we developed the concept of processing noise, which is the error in the system output due to errors in the deduced processing parameters. If there were no fluctuations in the ambient magnetic field or noise in the SQUID sensors, the processing noise would be set by computational accuracy (round off errors) or simplifying approximations for any algorithm that is used, and thus could be made arbitrarily small. In fact there are fluctuations in the ambient field, which result in finite processing noise. One can then differentiate among algorithms with respect to the manner in which the external field fluctuations translate into processing noise.

In Sec. IV a Least Squares processing algorithm is outlined. It is shown that such an algorithm is tractable only if the platform oscillations exceed some minimum value which depends on the magnitude of the external field fluctuations. The possibility of a uniformly increasing field, as would usually be encountered in the frame of a platform towed in the earth's field, is included explicitly in the algorithm. In its simplest version, the least squares algorithm requires a solution of 5 equations with 5 unknowns. When non-orthogonality terms are important, they can be incorporated in the least squares formalism in a straightforward (but tedious) way. We show that this requires inversion of a 10 x 10 matrix.

In Sec. V we summarize the results of extensive computer simulations of the least squares algorithm. The emphasis was on understanding how external fluctuations translate into processing noise. An important factor turns out to be the degree of correlation (in time) of both the external fluctuations and the platform oscillations. When the correlations are appreciable over the calibration interval used, the processing noise is comparable to the external fluctuations. (The calibration interval is essentially the delay between acquisition of triaxial data and output of scalar information.) Our computer simulations permitted generation of external fluctuations with a power spectral density ~(frequency)$^{-2}$, which corresponds to an infinitely long correlation time. This case was studied extensively, since it is likely to correspond to the situation in real life. It was found that a modification of the straightforward least squares processing which we call cumulative processing worked best in this case. The processing noise is found to depend on the correlation time τ_R of the platform oscillations, and can be much less than the external fluctuations at all frequencies if the calibration period is longer than τ_R.

An alternative procedure for determing the system parameters, known as adaptive processing, is discussed in Sec. VI. While it is simpler to implement than a least squares approach, it is found to have serious problems when used under realistic conditions. In particular, when the external field is assumed to have a uniformly increasing component a much more complicated

algorithm must be devised. Likewise it is shown that the convergence time (analogous to the calibration interval in least squares processing) is not well defined. These difficulties led us not to pursue the adaptive mode as extensively as the least squares.

The conclusions that can be formed on the basis of this work are given in Sec. VII. Basically we find that the cumulative processing algorithm that we developed should work well under conditions that would be encountered in practice. The main uncertainties lie with the hardware. On the one hand, platforms that might be used have not been adequately characterized, particularly with respect to maximum rotational slew rates and low frequency power spectral density. The only platform that looks as if it might be used with presently available SQUID systems is an underwater towed buoy.

There are, in addition, several questions that remain to be answered about the SQUID systems:

(1) It is not known whether the flux-counting/interpolation mode, which must be used in TRISCON processing, works as advertised outside of a laboratory environment.

(2) Non-linear or hysteretic magnetization effects in the construction materials could have a bad effect.

(3) It is possible that deviations from linearity, as well as other effects associated with motion of trapped flux, could be worse when a SQUID is operated in the flux-counting mode than in the feedback mode.

Finally it is recommended, in Sec. VIII, that an existing NRL triaxial SQUID system be modified to be used in a counting mode. By subjecting it to well-characterized rotations on a non-magnetic shake table (as is in development at Panama City) it should be possible to isolate various sources of error and verify feasibility under conditions approximating operational ones.

II. SQUID AND PLATFORM REQUIREMENTS

Before discussing specific algorithms, we should consider the dynamic range requirement on the sensors. This in turn depends on the angular excursions of the platform that can be expected. A study of the rotation spectrum of a suitable underwater towed buoy moving at speeds up to 7 kts was reported in Ref. 6. Over most of the frequency range studied the rotations were less than the resolution of the instruments used ($\sim 4\times10^{-5}/f$ rad/$\sqrt{\text{Hz}}$ below 10 Hz, and $\sim 2.5\times10^{-3}/f^{2.5}$ rad/$\sqrt{\text{Hz}}$ above 10 Hz, where f is the frequency). The major features that could be resolved were resonance peaks in the range 20-60 Hz with maximum rotations of $\sim 4\times10^{-6}$ rad/$\sqrt{\text{Hz}}$, and a component at frequencies below 2 Hz going like $10^{-4}/f^2$ rad/$\sqrt{\text{Hz}}$. The typical peak-to-peak excursions that occur in a 20 sec interval were of the order of 2×10^{-3} rad. A SQUID on such a buoy whose axis is oriented perpendicular to the earth's field would therefore see excursions as large as 100 γ.

A more recent report of the rotational motions of an airborne towed bird [9] shows p-p excursions as large as 0.06 rad. A study [10] of the possibility of reducing these motions found

that significant improvements should be possible using either passive or active stabilization techniques. The difficulties involved are considerable, however. For instance the "mass stablized" passive technique involves supporting the sensors with a spherical air bearing. The center of mass must be accurately centered relative to the bearing, or else up-and-down motions translate into rotations. In a SQUID system one has a continuously evaporating reservoir of liquid helium whose center of mass is ill defined and changing with time. An active system, with control surfaces servoed within a feedback loop, would face added problems due to stringent requirements on magnetic interference.

It previous work [1-5] it was assumed that the SQUIDs would be used in a feedback mode, and it was demonstrated that with platform excursions less than 2×10^{-3} rad the analog output would have sufficient linearity for use in a TRISCON mode. However, it is clear that all subsequent processing of the SQUID outputs must be done digitally. There seems to be little hope of obtaining an A-D converter with sufficient dynamic range to be useful in TRISCON processing. For instance if an 18 bit converter (the highest resolution that can be foreseen in the near future) was scaled to accomodate the maximum excursions of a towed buoy (100 γ), the least significant bit would correspond to $\sim 4 \times 10^{-4}\ \gamma$, which is much larger than the instrinsic device noise. In a presently available airborne towed bird the least significant bit would have to be $\sim 10^{-2}\ \gamma$.

An alternative mode of recording SQUID outputs, that makes

use of the inherently periodic nature of the SQUID response to magnetic field, has been known for some time.[11] Here one uses an up-down counter to directly count the number of flux quanta that have entered the SQUID ring. Between counts a feedback loop is activated that provides an analog interpolation corresponding to the fractional flux quanta in the ring. In a typical system one flux quantum corresponds to 0.05 γ. Since the interpolated signal lies between $\pm$ half a flux quantum, an A-D converter with only ~13 bits resolution would be required to have the least significant bit lie below instrument noise. This digitized interpolation could be digitally added to the suitably scaled contents of the up-down counter to yield a digitized output with essentially infinite dynamic range.

With a system of the sort just discussed, the critical requirement on platform rotations is no longer the amplitude but rather the maximum angular slew rate that can be expected. On the one hand, the settling time following a flux reset should be much less than the interval between resets. If the feedback loop gain has a frequency dependence $\sim f_m/f$, where f_m is the unity gain frequency, it turns out that the settling time is $\sim 2/f_m$. In currently available systems f_m can be as large as 20 KHz, yielding a settling time of $\sim 10^{-4}$ sec. The towed buoy of Ref. 6 exhibited peak rotation rates $\sim 6 \times 10^{-4}$ rad/sec. If the SQUID sensitivity is .05 γ/flux quantum, the period between resets would be $\geq 2 \times 10^{-3}$ sec, which is a fairly safe margin. Another possible source of error is the lag

between the actual feld at the SQUID and the analog output. It can be shown that when the field is changing at a rate $\dot{H}$, the difference between the output and the actual field is given by $\dot{H}/2\pi f_m$. Using the parameters listed above we find this offset can be as large as $2\times10^{-4}\,\gamma$ .However we shall show in a later section that the "time lag" offsets will not contribute very much to errors in the processed output.

The characteristic rotational slew rate of an airborne towed bird could not be determined from the data given in Ref. 9, but it is no doubt considerably greater than for an underwater buoy. On the other hand with the latest generation of ultra-low noise SQUIDs it should be possible to push f_m to ~300 KHz (the maximum f_m is determined by SQUID noise [12]).

The most important remaining questions about the flux-counting mode are whether the linearity, freedom from backlash, etc. will be as good as for the feedback mode. This uncertainty exists because rather large currents can be developed in the input flux transformer, in the former mode of a operation, whereas in the latter mode the current remains small. Only further experimental work can answer these questions.

III. PROCESSING THE SQUID OUTPUTS

Let $\underline{H}$ be the magnetic field in the reference frame of the SQUID sensors. Since this frame is subject to random, unknown rotations, the direction of $\underline{H}$ changes randomly and has no significance. The three SQUID outputs V_1, V_2, V_3 can formally

be represented by a vector $\underline{V}$. The axes are nominally aligned with an ideal orthogonal coordinate system, and the gains of the three systems are adjusted to be nearly identical. There exists a matrix of the form $\underline{\underline{I}}+\underline{\underline{D}}$ that transforms $\underline{V}$ into a vector measured along the ideal axes. Here $\underline{\underline{I}}$ is the identity matrix, and $\underline{\underline{D}}$ contains all the deviations from ideal: the diagonal terms represent relative deviations of the gain of the three sensors from their nominal value, and the off-diagonal terms are of the order of the angular deviations of the axes from the ideal coordinate system. A prototype system [2] had deviations from orthogonality no greater than 2×10^{-4} rad. It seems plausible that the gains could be matched to about the same relative precision.

We now suppose that at t=0 the sensors are turned on (or equivalently, all subsequent readings are subtracted from those at t=0). If the components of $\underline{H}$ are measured along the set of ideal axes mentioned above, we have

$$\underline{H} = \underline{H}(0) + (\underline{\underline{I}}+\underline{\underline{D}})\underline{V}. \tag{1}$$

Likewise the change H in the magnitude of $\underline{H}$ after t=0 is defined:

$$|\underline{H}| = |\underline{H}(0)| + \Delta H. \tag{2}$$

After squaring Eqs. 1 and 2 and equating the results, we find

$$\Delta H = (2\underline{A}\ \underline{V} + [(\underline{\underline{I}}+\underline{\underline{D}})\underline{V}]^2)/2|\underline{H}(0)|, \tag{3}$$

where $\underline{A} = (\underline{\underline{I}}+\underline{\underline{\tilde{D}}})\underline{H}(0)$. ($\underline{\underline{\tilde{D}}}$ is the transposed matrix.) In Eq. 3 a correction to ΔH of the order of $(\Delta H)^2/|H(0)|$ has been neglected. Since $|H(0)|$ is approximately the earth's field H_e, and ΔH could not conceivably be greater than 10^{-3} H_e, this approximation is very good.

According to Eq. 3 the scalar quantity ΔH can be deduced from the SQUID outputs if $\underline{H}(0)$ and $\underline{\underline{D}}$ are known. A great simplification would result if we were relieved of the necessity of explicitly evaluating $\underline{\underline{D}}$. Accordingly we consider the following approximation of Eq. 3:

$$\Delta H' = (\underline{A}\ \underline{V} + V^2/2)/|\underline{A}| \qquad (4)$$

Note that Eq. 4 contains only an <u>implicit</u> dependence on $\underline{\underline{D}}$ via the vector $\underline{A}$. We will show that $\underline{A}$ can be determined with adequate precision even when $\underline{\underline{D}}$ is not explicitly known. Assuming that $\underline{A}$ has been correctly determined, there remain the following errors that result when Eq. 4 is used instead of Eq. 3:

(1) $\Delta H'$ differs by a constant factor $|\underline{H}(0)|/|\underline{A}|$ from the true value ΔH. This amounts to an uncertainty in the overall proportionality factor between system output voltage and magnetic field of the order of some linear combination of elements in $\underline{\underline{D}}$, which should be acceptable in any application.

(2) The lowest order error in $\Delta H'$ due to $\underline{\underline{D}}$ is given by

$$\delta H = \Delta H - \Delta H' \cong \underline{V}\ (\underline{\underline{D}}\underline{V})/H_e. \qquad (5)$$

The magnitude of $\underline{V}$ is primarily governed by rotations of

the platform, $V \sim \Theta H_e$. Calling d the appropriate average of the elements in $\underline{\underline{D}}$, we have

$$\delta H \sim \Theta^2 H_e d. \qquad (6)$$

Using $d = 2\times10^{-4}$, $\Theta(\text{peak}) = 10^{-3}$ rad as is the case for the towed buoy, we find $\delta H(\text{peak}) \sim 10^{-5}\ \gamma$. In a 10 Hz bandwidth the instrument noise ($10^{-5}\ \gamma/\sqrt{\text{Hz}}$) would mask such errors by a factor ~ 3.

(3) The technique for determining $\underline{A}$, which will be discussed in the next section, results in an incorrect value when $\underline{\underline{D}} \neq 0$. In Appendix A the magnitude of this error is estimated, and the resulting errors in $\Delta H'$ are evaluated. Briefly, it is shown that there is a relative error in the magnitude of $\underline{A}$ given by a linear combination of elements of $\underline{\underline{D}}$. Such an error only has an effect on the second term in Eq. 4, and can be shown to contribute an error of the same order as that of Eq. 6. The error in $\Delta H'$ due to errors in the direction of $\underline{A}$ is shown to be $\sim \Theta^3 H_e d$, which is negligible in comparison with previously discussed errors.

In conclusion, we find that as long as the angular excursions of the sensor platform do not exceed $\sim 10^{-3}$ rad, it is possible to ignore deviations from orthogonality of the order of 2×10^{-4} rad and less. In subsequent sections we therefore assume $\underline{\underline{D}}=0$, and consider the problem of determining $\underline{A}$. An extension of the processing to take account of finite $\underline{\underline{D}}$ will be outlined in Sec. IV.

We assume that there is no input to our processing system other than the sensor readouts $\underline{V}$. Our problem is to determine $\underline{A}$ using a sequence of values of $\underline{V}$ resulting from rotations of the platform. It is illuminating to consider this problem in the limit $\Delta H'=0$, that is when the total field remains constant during the rotations. In this case the vector $\underline{V}$ has its origin on the surface of a sphere, and its tip traces out a path on the surface. The problem is to locate the center of this sphere (at $-\underline{A}$). In principle any three points on the surface are sufficient to locate the center. In practice there are uncertainties in the readings of $\underline{V}$, and a better approach is to use some sort of average of the information contained in many samples. Even so, there will be a finite error in the computed value of $\underline{A}$, and this will translate into errors in $\Delta H'$ calculated from Eq. 4. The magnitude of these errors constitutes some sort of figure of merit of any scheme used to determine $\underline{A}$; we will refer to this component of uncertainty as the processing noise in the system output.

In Eq. 4 $\Delta H'$ is not in fact equal to zero even if $\underline{A}$ is known exactly. We can identify the following contributions to $\Delta H'$:

(1) Sensor Noise: If we call $\underline{V}_N$ the contribution to $\underline{V}$ due to noise in the SQUIDs, it can easily be shown that the resulting contribution to $\Delta H'$ is just the projection of $\underline{V}_N$ along $\underline{A}$, which we can call V'_N. Note that the rms average of V'_N is the same as the noise in a single channel, $\sim 10^{-5}\ \gamma/\sqrt{\text{Hz}}$.

(2) Geomagnetic Noise: In the frequency range of interest this is mostly due to lightning strikes, whose electromagnetic energy is propagated over great distances. It is quite variable from day to day, and we shall use values described as "moderate" levels in Ref. 13: ~ $10^{-3}\gamma/\sqrt{Hz}$ around 1 Hz, falling to ~ $3\times10^{-4}\gamma/\sqrt{Hz}$ at frequencies above 20 Hz. ("High" levels can be 50 times greater.) A significant fraction of the total energy is in the form of narrow, large amplitude spikes due to nearby lightning. This means that some of this noise can be removed with non-linear processing techniques [13] or by visual inspection. Nevertheless it is clear that geomagnetic noise will completely dominate sensor noise discussed above. This remains true in the frequency range of interest even at depths 200 m beneath the sea surface; the noise is attenuated by a factor ~ 2 at 1 Hz, ~ 10 at 10 Hz.[14] However, the spikes will be almost completely removed.

(3) The gradient in the earth's field, which can be as large as 10^{-2} γ/ft, will result in a linear increase of $\Delta H'$ with time, proportional to the velocity at which the platform is being towed. Fluctuations in altitude or velocity will contribute to the noise in $\Delta H'$, probably at a level intermediate between (1) and (2) above.

(4) Signals: The processing system has no way of distinguishing components of $\Delta H'$ which may be of interest to the operator from the noise sources mentioned above - that is, we are assuming that one has no more a priori knowledge of the form of "signals" than of noise.

The above contributions to $\Delta H'$ lead to the following version of Eq. (4):

$$H_x(t) - H_x(0) + \dot{H}t = (\underline{A}\ \underline{V} + V^2/2)/|A|. \qquad (7)$$

Here all of the noise and signal components are lumped together as H_x. The average of H_x is assumed to be zero. $H_x(0)$ must be included explicitly since the definition of $\underline{V}$ implies that the RHS is zero at t=0.

IV. DETERMINATION OF THE PROCESSING PARAMETERS BY LEAST SQUARES

Equation 7 can be rewritten as follows:

$$H_x(t) = (\sum_{i=1}^{5} A_i V_i + V^2/2)/|A|. \qquad (8)$$

Where we have defined $A_4 = |A|\ H_x(0)$, $V_4 = 1$, $A_5 = -|A|\dot{H}$, $V_5 = t$. The remaining terms (i=1,2,3) are vector components. The least squares solution for the parameters A_i is defined as that which minimizes the mean square average of the RHS of Eq. 8 for a sequence of $\underline{V}$'s. The least squares solution for the A_i should tend to the correct values as the averaging period becomes large, provided that H_x is not correlated with the platform motions. Since this is presumeably true both for "signals" and "noise" we feel that no generality is lost in combining the two. Formally, we require that

$$\frac{\partial S}{\partial A_i} = 0,\ i = 1,2,\ldots 5 \qquad (9a)$$

where $$S = \overline{(\sum A_i V_i + V^2/2)^2}/A^2 \qquad (9b)$$

and $$A^2 = A_1^2 + A_2^2 + A_3^2. \qquad (9c)$$

The bar signifies a time average.

Equations 9 can be rewritten in terms of the elements of a 5x5 matrix $\underline{M}$ and a 5-componment vector $\underline{B}$:

$$\sum_{j=1}^{5} M_{ij}A_j - SA_i = B_i \quad i=1,2,3, \tag{10a}$$

$$\sum_{j=1}^{5} M_{ij}A_j = B_i \quad i=4,5 \tag{10b}$$

where $$M_{ij} = \overline{V_i V_j} \tag{10c}$$

$$B_i = -\overline{V_i V^2}/2 \tag{10d}$$

Note that Eqs. 10a and 10b are <u>not</u> linear in $\underline{A}$, since S is itself a complicated function of A via Eq. 9b. We have not found any straightforward means of solving Eqs. 10 in the general case. In Appendix B we show that the importance of the term proportional to S in (10a) is governed by the dimensionless parameter x:

$$x^2 = H_x(\text{rms})/(H_e\overline{\theta^2}). \tag{11}$$

When x exceeds some critical value the full non-linear set of equations must be solved. However, for sufficiently small x the non-linear term can be dropped with no significant loss of accuracy. Computer simulations, described in a later section, show that the critical value of x lies between 0.3 and 0.5, depending on other system parameters. Reasonable estimates for H_x(rms) are $10^{-2}\ \gamma$ in air, $5\text{x}10^{-4}\ \gamma$ at a depth of 200m, both assumming a moderate level of atmospheric noise. Then the linearized version of Eqs. 10 can only be used when θ_{rms} is greater than $\sim 10^{-3}$ rad

and 2×10^{-4} rad, respectively. This criterion is certainly met for airborne towed birds, and is marginally satisfied for an underwater towed buoy.

The first algorithm we have considered breaks the input data (the V_i) into blocks of N samples. The matrix elements M_{ij} and B_i are accumulated within each block, and the linearized version of Eqs. 10a, 10b is inverted to obtain an estimate of the A_i. Finally, the original data (which were stored in memory) are used to compute $H_x(t)$ via Eq. 8 for the whole sequence of N samples. This is just the residual of the least-squares fit, and can be divided into two parts: (1) the actual signal and noise components that were present, and (2) errors due to deviations of the A_i from their true values. We refer to the latter as "processing noise". It turns out that the processing noise scales linearly with $H_x(\text{rms})$, and consequently has no analog in a scalar magnetometer. (The instrument noise of the latter would not be affected by the level of external geomagnetic noise.)

It can be argued that the processing noise need only be somewhat less than the external noise. However, two properties of geomagnetic noise imply that instrument sensitivities well below the ambient noise levels could be used to advantage:

(1) It is non-Gaussian in its amplitude distribution, as a result of the "spike" features. A non-linear noise processor described in Ref. 13 was able to effectively remove these spikes, resulting in a 10-20 dB reduction in the "effective" geomagnetic noise level. Such a scheme would ultimately be limited by the

processing noise component (or sensor noise, if it is greater) of the TRISCON output.

(2) It is highly correlated in space. This means that the outputs of two separated magnetometers could be combined in such a way as to significantly reduce the geomagnetic component but retain full sensitivity for the "signal" component. Again, it is desirable that the overall instrument noise level be well below H_x(rms).

It should be noted that with the algorithm outlined above one must wait N sampling intervals (plus the computer time needed to invert $\underline{\underline{M}}$, etc.) between initial data acquisition and display of the processed results. Hence, it cannot strictly be said to operate in real time, even though the delay might not be more than half a minute. An approach was outlined in Ref. 7 (and implicitly in Ref. 4) that gives an output in real time. The idea is to have an initial calibration period in which one calculates $\underline{A}$. This $\underline{A}$ is then used to calculate ΔH for all subsequent readings of $\underline{V}$. The most significant problem with this approach is that there is no room for adjustments to be made in response to changes in the actual system parameters (especially changes in H due to fluctuations in towing speed). It will also be shown below that even without such changes the overall processing noise can be significantly greater when an initial determination of the parameters is used with subsequent data.

To conclude the section on least squares processing, we will outline the procedure by which this general technique can

be extended to more complicated situations. An obvious example is the possibility that the non-orthogonality and gain non-uniformity cannot be ignored. In conversations with the vendor of a previous system, we were informed that a relaxation of the requirement that these terms be less than 10^{-4} could reduce the price of a system by a factor of 2. It would then be necessary to include these terms in the processing. It is convenient to rewrite Eq. 3 as follows:

$$\Delta H \cong (\underline{A}\,\underline{V} + \underline{V}\,\underline{\underline{E}}\,\underline{V} + V^2/2)/A \tag{20}$$

where $2\,\underline{\underline{E}} = \underline{\underline{D}} + \underline{\underline{D}} + \underline{\underline{\tilde{D}}}\,\underline{\underline{D}}$. (21)

The error matrix $\underline{\underline{D}}$ has 5 independent terms; 2 associated with the lack of gain uniformity (diagonal terms) and 3 associated with deviations from orthogonality (off-diagonal terms) [7]. The same is true of $\underline{\underline{E}}$ we can, for instance, take it to be a symmetric matrix with one of the diagonal elements equal to zero. Suppose we label the independent elements, in no particular order, A_6 through A_{10}. As before, we define the error function $S = \overline{\Delta H^2 A^2}$:

$$S = (\sum_{i=1}^{10} A_i f_i + V^2/2)^2 \tag{22}$$

The functions f_i were defined previously for $i = 1\text{-}5 \cdot f_i = V_i$ for $i = 1,2,3$; $f_4 = 1$, $f_5 = t$. If we had defined $A_6 = E_{11}$, $A_7 = E_{12} = E_{21}$, etc. we would have $f_6 = V_1^2$, $f_7 = 2V_1V_2$, and so on. Minimization of S is formally similar to the set of linear equations (10), with $M_{ij} = \overline{f_i f_j}$ and $B_i = -\overline{f_i V^2}/2$. Note

that the computational requirements have significantly increased; there are now 55 independent elements of $\underline{\underline{M}}$ to be evaluated (compared to 15 when orthogonality errors are ignored), and many of them involve 4th order products of SQUID readings. Solution of the set of equations by the method of Gaussian Elimination [15] requires of the order of $2N^3/3$ floating point multiplications - ie, around 8 times more operations when N = 10 than when N = 5 (N is the order of the matrix of coefficients).

Another interesting possibility (suggested by C. Sinex) is to simultaneously process the sensor readings of two separate triaxial systems, mounted on individual platforms. If they are separated by no more than, say, a mile or so, we would expect the geomagnetic component of the outputs to be nearly identical. (Geomagnetic noise is correlated over large distances.) It is therefore reasonable to construct the error function

$$S = A^2 \overline{(\Delta H_1 - \Delta H_2)^2} = \overline{\left(\sum_{i=1}^{5} (A_{1i}V_{1i} - A_{2i}V_{2i}) + (V_1^2 - V_2^2)/2 \right)^2}. \qquad (23)$$

Here the subscripts (1) and (2) refer to the components of the different systems, and we have ignored deviations from orthogonality. Equation 23 can obviously be cast into a form similar to (22) by appropriate identification of terms, and a least squares solution involving a 10x10 matrix of coefficients can be simultaneously obtained for the offsets of the two systems. This requires significantly more computation than would be involved in independently processing each system. However, it should yield a more accurate determination of the

(to the extent that ΔH_1 and ΔH_2 are correlated).

V. COMPUTER SIMULATIONS OF LEAST SQUARES PROCESSING

Computer simulations of the algorithm suggested above are of course desireable simply to demonstrate that it works. Beyond that, simulations can be very useful in characterizing the way that external noise translates into processing noise. The connection between these two is quite non-linear and not easily subject to mathematical analysis. A large portion of the simulations therefore were concerned with determination of the frequency spectrum of the processing noise as a function of the spectrum of external noise, processing algorithm, etc.

Many of the details of the computation techniques are given in Appendix C. A total field consisting of the earth's field, 5×10^4 γ, a randomly varying external field H_x, and a linearly increasing component was assumed. A series of random rotations were generated, and the SQUID readings that would result from these rotations were computed. It was assumed that the SQUID axes were perfectly orthogonal to one another. The rotations, as well as H_x, were derived from a random number generator with a normal distribution, and their power spectral density had the Lorentzian form $\sim [1 + (\omega\tau)^2]^{-1}$. Here ω is the angular frequency, and τ is a characteristic correlation time. By varying τ we could cover the range of statistics from uncorrelated (τ=0) to a random walk ($\tau \gg T$).

The simulated SQUID data were analyzed using the least squares algorithm discussed above. The processing noise H_{pn} associated with each point was found by subtracting H_x from the residual of the least-squares fit. For each calibration interval (N points) the deviations of the calculated A_i from their true values were evaluated. In order to get adequate statistics for the rms average of these quantities it was sometimes necessary to use as many as 50,000 points in the simulation.

In Fig. 1 we show how the processing noise depends on the parameter x for a few values of the correlation times, all with N=100. We see that there is a sharp increase in the normalized processing noise, when x exceeds some critical value, which does not depend much on the magnitude of the correlation times. For x less than this critical value (0.3-0.5), H_{pn} is proportional to the driving noise H_x.

Figure 2 shows the dependence of $H_{pn}(\text{rms})/H_x(\text{rms})$ on the number of points N used in the fit, for various correlation times of the noise and rotations. A number of important conclusions can be drawn from the graph: When N=5 we find $H_{pn}(\text{rms}) = H_x(\text{rms})$ under all conditions. This is an artifact of the definition of H_{pn} and does <u>not</u> mean that one has an adequate signal/noise ratio. It can be shown that the least squares formalism for N=5 reduces to the requirement that the RHS of Eq. 8 be zero for each of the 5 values of $\underline{V}$. The output of the processor will be identically zero at all times, demonstrating

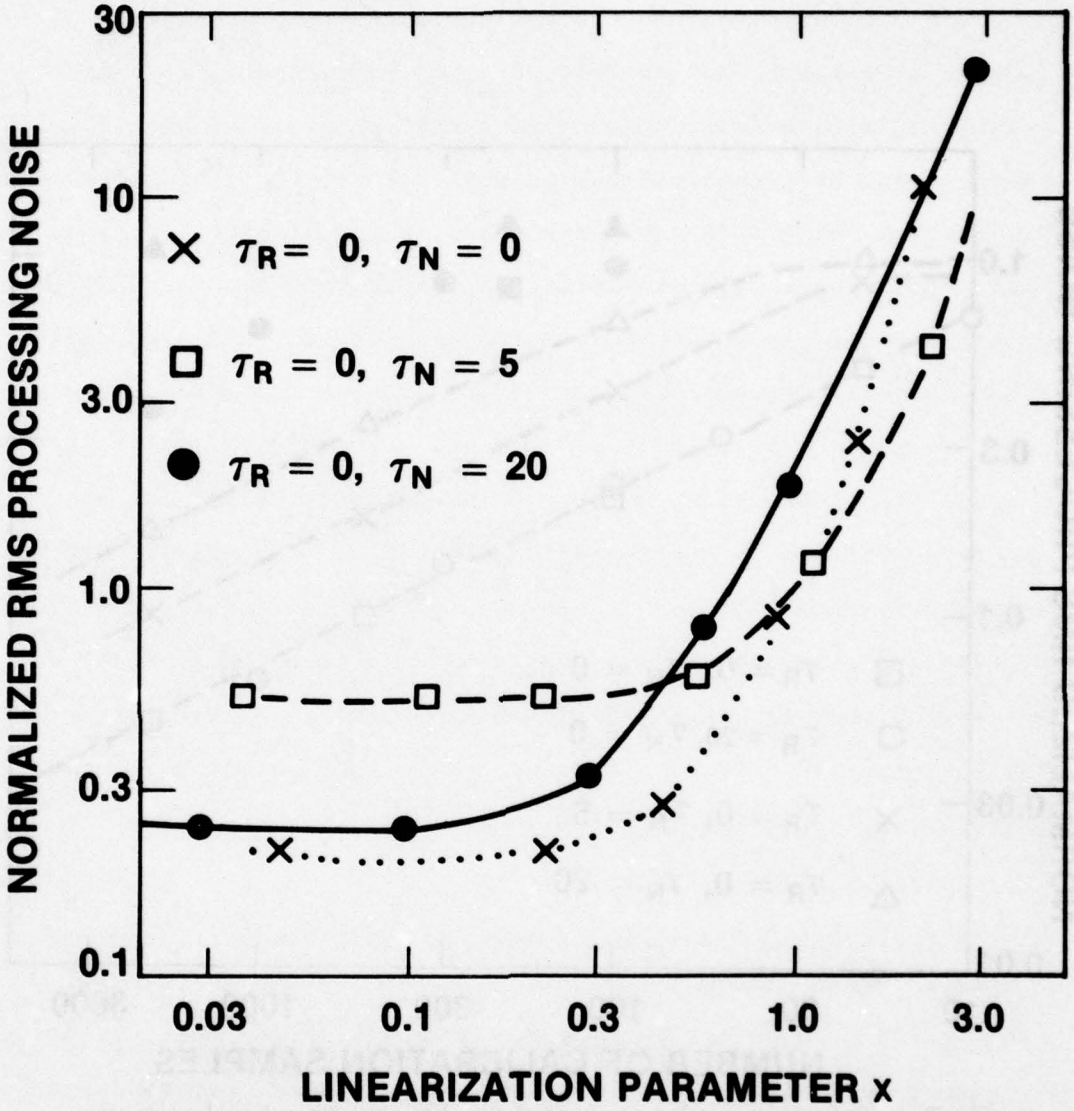

Fig. 1 — A plot of the rms processing noise, normalized to the rms external noise, as a function of the parameter x (defined in Eq. 11). The "residual" processing mode was used. τ_R and τ_N are the correlation times for the platform rotations and external noise, respectively, in units of the sampling interval.

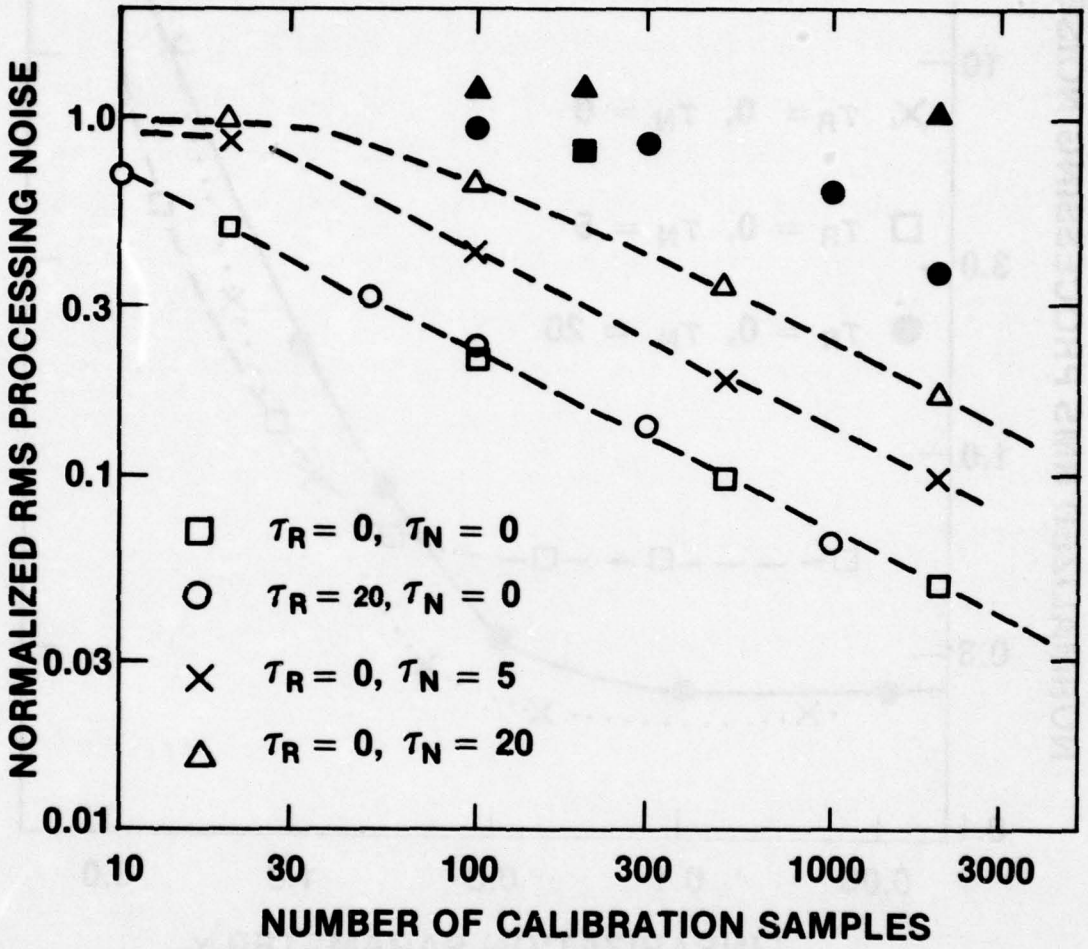

Fig. 2 — The rms processing noise, normalized to the rms external noise, as a function of the number of samples used in each calibration interval. The "residual" processing mode was used, and τ_R and τ_N are defined as in Fig. 1. The open points correspond to the algorithm discussed in the text, and the solid points result when the "initial offset" fitting parameter is omitted. The linear portions of the dashed lines follow Eq. 12.

that 5 equations in 5 unknowns can be solved - but not providing us with useful information. Of course, one might be willing to sacrifice information about H_x during an initial calibration interval if the computed values of the A_i could be used with subsequent SQUID data to calculate H_x. This is essentially the approach used in Ref. 7. Some criticisms of this general approach have already been given - we mention here in addition the fact that with such a small number of samples the determination of the A_i is not very accurate, and thus the processing noise will be quite high. In some simulations of this case [8] at APL by Dr. Sinex it was found that the processing noise is usually much greater than the external noise.

In the context of the algorithm used in this work, H_{pn} is meaningful only when N>>5. We see in Fig. 2 that the processing noise falls monotonically with increasing number of points used in the fit, eventually approaching a dependence that is well approximated by:

$$H_{pn}(\text{rms}) \cong H_x(\text{rms}) \left[\frac{5\tau_N + 10}{2N}\right]^{1/2} . \qquad (12)$$

Here τ_N is the correlation time of the noise in units of the sampling interval Δt. It is somewhat more illuminating to write this equation in terms of actual times: $T = N\Delta t$ is the time interval of each least-square fit, and $T_N = \tau_N \Delta t$ is the correlation time of the noise:

$$H_{pn}(\text{rms})/H_x(\text{rms}) \cong \left[\frac{T_N/2 + \Delta t}{T/5}\right]^{1/2} \qquad (13)$$

This equation can be used to help decide on the optimum sampling interval, for a given correlation time and calibration interval: Δt should be less than $T_N/2$, but need not be significantly less. On the other hand, a longer Δt places less stringent requirements on the computing speed, memory requirements, etc.

Previous discussions of a least-squares approach [3-5, 8] have ignored the term A_4 (the initial offset) in Eq. 8. This has the advantage, of course, of reducing the order of the matrix that must be inverted; however, our simulations of the simplified algorithm show that the resulting processing noise is much greater than when the full algorithm is used. Some representative results of these simulations are also shown in Fig. 2.

The results for H_{pn} are independent of the assumed rate of change of the total field, up to rates at least as large as 0.03 γ/sample. It is not known what mechanism sets this limit.

It is helpful in interpreting the results of Fig. 2 to prepare a sort of error budget, wherein contributions to H_{pn} of specific errors in the A_i are separately evaluated. Referring to Eq. 8, we make the following breakdown:

(1) The error $\underline{\Delta m}$ in the <u>direction</u> of $\underline{A}$ results in a mean-square contribution to H_{pn} (here $\underline{m}$ is a unit vector in the direction of $\underline{A}$):

$$H_{pn}^2(1) = (\Delta m)^2 \overline{V^2} = (\Delta m)^2 H_e^2 \overline{\theta^2}. \qquad (14)$$

(2) An error ΔA in the <u>magnitude</u> of $\underline{A}$ leads to a contribution from the second term in (8):

$$H_{pn}^2(2) = \frac{(\Delta A)^2}{A^4}\left(\frac{\overline{V^4}}{4}\right) = 3\,(\Delta A)^2\,[\overline{\theta^2}]^2. \qquad (15)$$

(3) The error in A_4 (the initial offset) contributes directly to H_{pn}:

$$H_{pn}^2(3) = (\Delta A_4)^2/A^2. \qquad (16)$$

(4) An error in the rate of change of ΔH, when averaged over the N samples, yields:

$$H_{pn}^2(4) = (\Delta A_5)^2\, N^2/3A^2. \qquad (17)$$

The simulation program computed the mean square errors in $\underline{m}$, A, A_4, and A_5, as well as the overall processing noise, for a large number of calibration intervals. In Table I we list the corresponding expected contributions to H_{pn}^2 as calculated from Eqs. 14-17. When the driving noise H_x is uncorrelated (τ_N=0), all of the terms are roughly of the same magnitude. The sum of the individual contributions is greater than the overall processing noise. The discrepancy between the "whole" and the sum of its parts becomes more pronounced as the correlation time of the rotations increases. One can see how this might happen as follows: in a system with a long correlation time the vector $\underline{V}$ might trace out something like a simple arc on the surface of a sphere during a calibration period. If $\underline{\Delta m}$ is predominantly perpendicular to this arc it will not contribute much to H_{pn} - certainly not as much as Eq. 14 suggests. On the other hand the locus of points $\underline{V}$ will cover a patch of the sphere more uniformly if

TABLE I

Source of error	$\tau_R = 0$ $\tau_N = 0$	$\tau_R = 20$ $\tau_N = 0$	$\tau_R = 0$ $\tau_N = 5$	$\tau_R = 0$ $\tau_N = 20$
Direction of $\underline{A}$	.046	.12	.029	.017
Magnitude of $\underline{A}$	.031	.10	.023	.015
Initial offset (A_4)	.063	.078	.34	.78
Rate (A_5)	.039	.11	.37	.75
Overall $\overline{H_{pn}^2}/\overline{H_N^2}$	.050	.055	.19	.42

Mean-square errors in the system parameters determined by least squares, for various values of the correlation times τ_R and τ_N (of the rotations and noise, respectively) normalized to the sampling interval. The numbers given are the mean square average of the contribution each error would make to the overall processing noise, using Eqs. 14-17, normalized to the mean square input noise. In all cases N = 100, x < 0.1.

the correlation time of the rotations is small (all other things being equal). To achieve the same average contribution to H_{pn} the latter case requires a smaller magnitude of $\underline{\Delta m}$. These observations underscore an important point: it is not the errors in the A_i that matter, but rather the errors in the overall output of the processor.

If one were to use the values of A_i determined from an initial "calibration" data sequence to compute ΔH for subsequent readings, it is likely that the mean-square processing noise would eventually be the sum of the individual contributions outlined in Table I. Using the example of the previous paragraph, $\underline{V}$ would eventually become parallel to $\underline{\Delta m}$, and Eq. 14 would correctly describe the the contribution of the error in direction of $\underline{A}$ to H_{pn}, as would Eqs. 15-17. The total mean square processing noise would then be of the order of the sum of the individual components, which is significantly greater than when new values of the A_i are computed during each calibration interval.

It can also be seen in Table I that as τ_N gets large the total processing noise is dominated by errors in A_4 and A_5. These errors contribute primarily to low frequency components of H_{pn}. In practice one may only be interested in frequencies above some lower limit; for instance if a detector moving at velocity v passes at closest approach within a distance d of a target dipole, 85% of the signal energy is at frequencies above $v/2\pi d$. It is also possible that the effective correlation time

for geomagnetic noise might be much greater than any reasonable calibration interval. The data of Fig. 2 imply that in this case the processing noise can never be less than the external noise.

The residual of the least-squares fit, which we have taken to be the output of the processing system, is by definition the best estimate of H_x over the entire sensor bandwidth. The considerations of the previous paragraph suggest that a best estimate of H_x above some lower frequency limit is more desireable. The following approach was therefore considered: The processed output within each calibration interval is given by:

$$H_p(t) = H_p(0) + (\underline{A}\,\underline{V} + V^2/2)/|A| \qquad (18)$$

$H_p(0)$ is *not* the fitted initial offset ($A_4/|A|$) but rather is chosen to make H_p continuous from one calibration interval to the next. This is accomplished by using the parameters of the previous interval to calculate H_p for the first point (defined as t=0) of the current interval. We will use the term cumulative to identify this type of processing, since the output within each calibration interval builds upon the previous one. Notice that the processing errors also accumulate - the error in the initial offset in each calibration is propagated, along with an additional error due to errors in the calculated $\underline{A}$, into the next calibration period. Thus the difference between the processed output and the true external field follows a random walk process, and grows without limit. This should lead to a low-frequency dependence

of the spectrum of the processing noise that goes like f^{-2} or faster. Note also that H_p includes the linear increase in total field, in contrast to the residual. For these reasons H_p would probably be passed through a high-pass filter prior to further analysis.

The cumulative processing scheme has been simulated on a computer in a similar manner as for the residual processing scheme. Since the total processing noise is unbounded, the frequency dependence of the processing noise must be calculated. A particularly interesting case is that where the correlation time of the external noise is much greater than the calibration interval T. Figures 3 and 4 show the power spectrum of the processing noise in this limit for a series of sampling rates. The following general conclusions can be drawn:

(1) At very low frequencies the processing noise more or less tracks the external noise - that is, depends on frequency roughly as f^{-2} (or slightly faster). It can lie well below the actual external input down to frequencies much less than T^{-1} - ie, the cummulative processing output is meaningful even for features that extend over tens of calibration periods.

(2) As the sampling rate $(\Delta t)^{-1}$ increases the processing noise is reduced (keeping T fixed). This is intuitively reasonable, since higher sampling rates provide more information to work with. However once Δt is comparable to the correlation time of the platform rotations, the improvements with

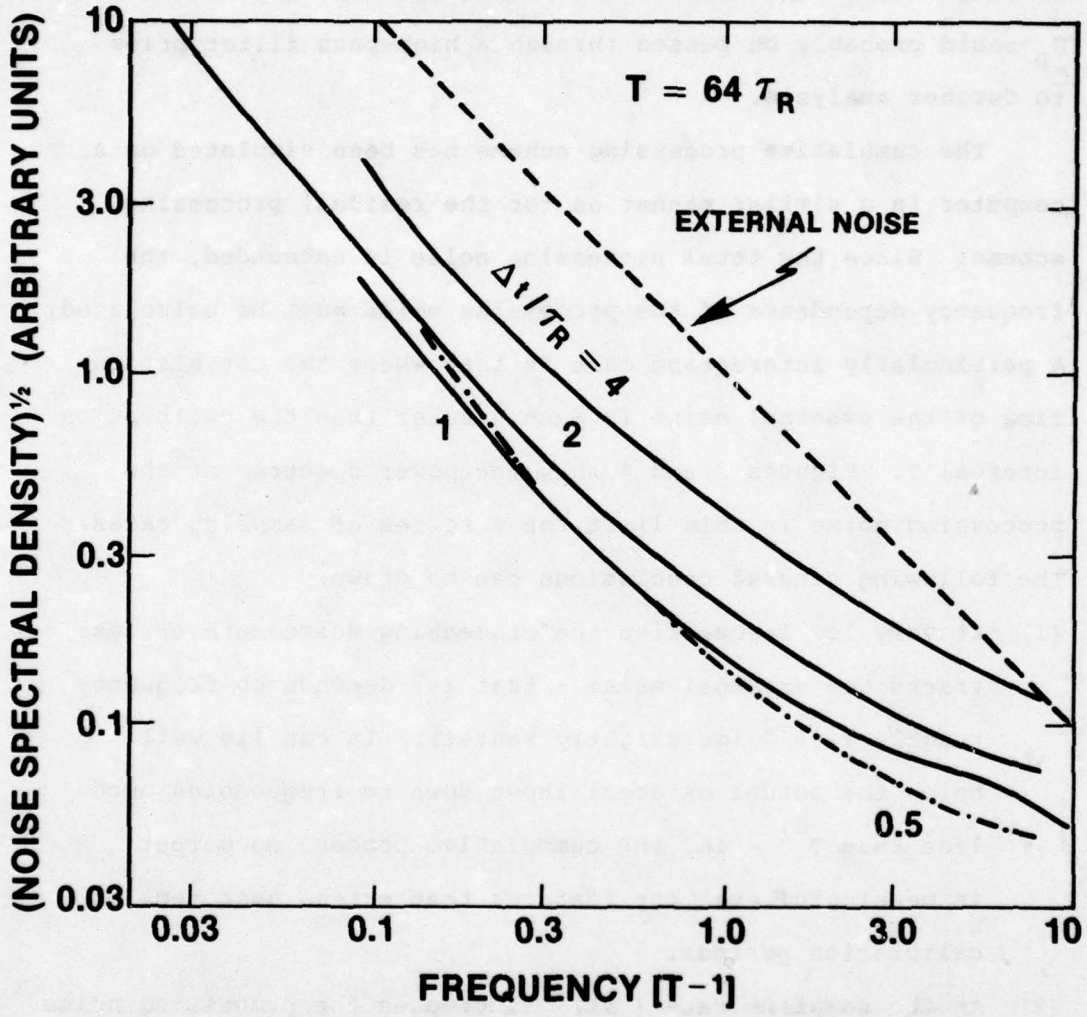

Fig. 3 — A plot of the power spectral density (PSD) of the processing noise, as a function of frequency, for the "cumulative" processing mode. The external noise is assumed to have a PSD $\sim f^{-2}$ - ie, it has a correlation time much longer than the inverse of any frequency of interest. Frequency is measured in units of 1/T, where T is the calibration interval. Results are shown for various sampling rates $(\Delta t)^{-1}$, where Δt is normalized to τ_R, the correlation time of the platform rotations.

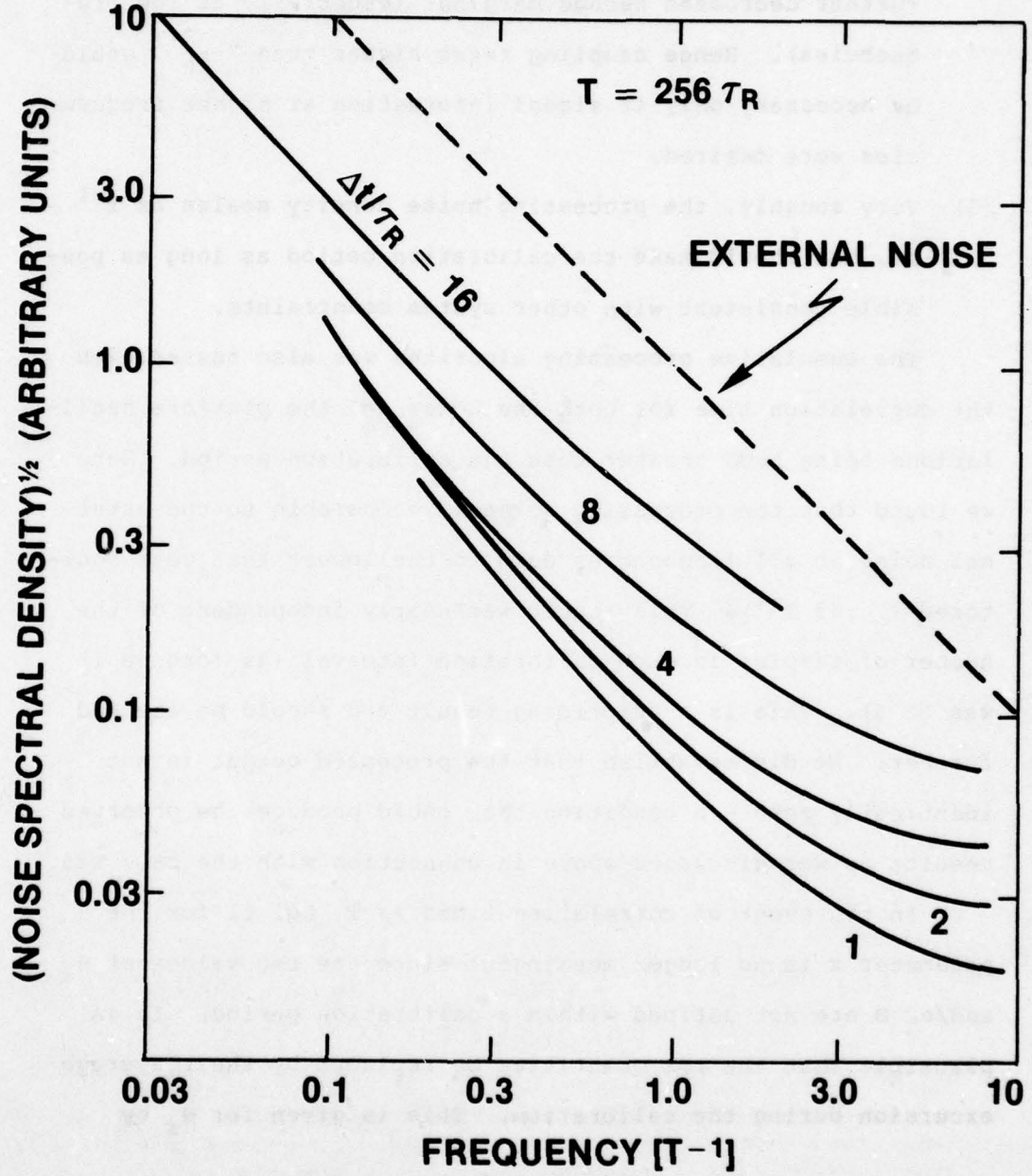

Fig. 4 — Similar to Fig. 3, except that a calibration interval 4 times larger is assumed

further decreases become marginal (especially at low frequencies). Hence sampling rates higher than $\sim \tau_R^{-1}$ would be necessary only if signal information at higher frequencies were desired.

(3) Very roughly, the processing noise density scales as T^{-1} - ie, one should make the calibration period as long as possible consistent with other system constraints.

The cumulative processing algorithm was also tested with the correlation time for both the noise and the platform oscillations being much greater than the calibration period. Here we found that the processing noise is comparable to the external noise at all frequencies down to the lowest that were monitored ($\sim .03\ T^{-1}$). This result was nearly independent of the number of samples in each calibration interval (as long as it was >> 5). This is a surprising result and should be checked further. We did establish that the processed output is not identically zero - a condition that could produce the observed results as was discussed above in connection with the case N=5.

In the event of correlation times >> T. Eq. 11 for the parameter x is no longer meaningful since the rms values of H_x and/or Θ are not defined within a calibration period. It is plausible that the rms quantities be replaced by their average excursion during the calibration. This is given for H_x by

$$(\Delta H_x)_{rms} = \sqrt{2T}\,\pi\,(\sqrt{G_x(f)\,f}), \tag{19}$$

where $G_x(f) \sim f^{-2}$ is the PSD of H_x. Note that the average

excursion increases as $T^{1/2}$, as is characteristic of a random walk process. It was found that the cumulative processing scheme breaks down at $x > 0.3$, in qualitative agreement with the results of Fig. 1, when the correlation times of both the rotations and noise are >> T. Here x is defined in terms of mean excursions, rather than rms values, as was discussed above.

Finally, we have compared the cumulative and residual processing modes in a situation where both can be used - ie, where the calibration interval is greater than any correlation times. An example is given in Fig. 5. Note that the residual has lower noise only at frequencies $< 0.1\ T^{-1}$, for the particular parameters used.

VI. ADAPTIVE DETERMINATION OF THE PROCESSING PARAMETERS

We will use the term adaptive processing to describe any scheme in which the parameters A_i are continuously updated according to some algorithm. The details of this "feedback" algorithm can be varied indefinitely, but there are some universal features of adaptive processing that are independent of the specific algorithm. An initial estimate of the A_i must be supplied; they will then decay toward their correct values more or less exponentially. Quite generally, when there is noise in the total external field it will translate into errors in the corrections made in the A_i. As a result the offset parameters will fluctuate randomly about their correct values after the initial decay is over, and there will be errors in the processed output of the system.

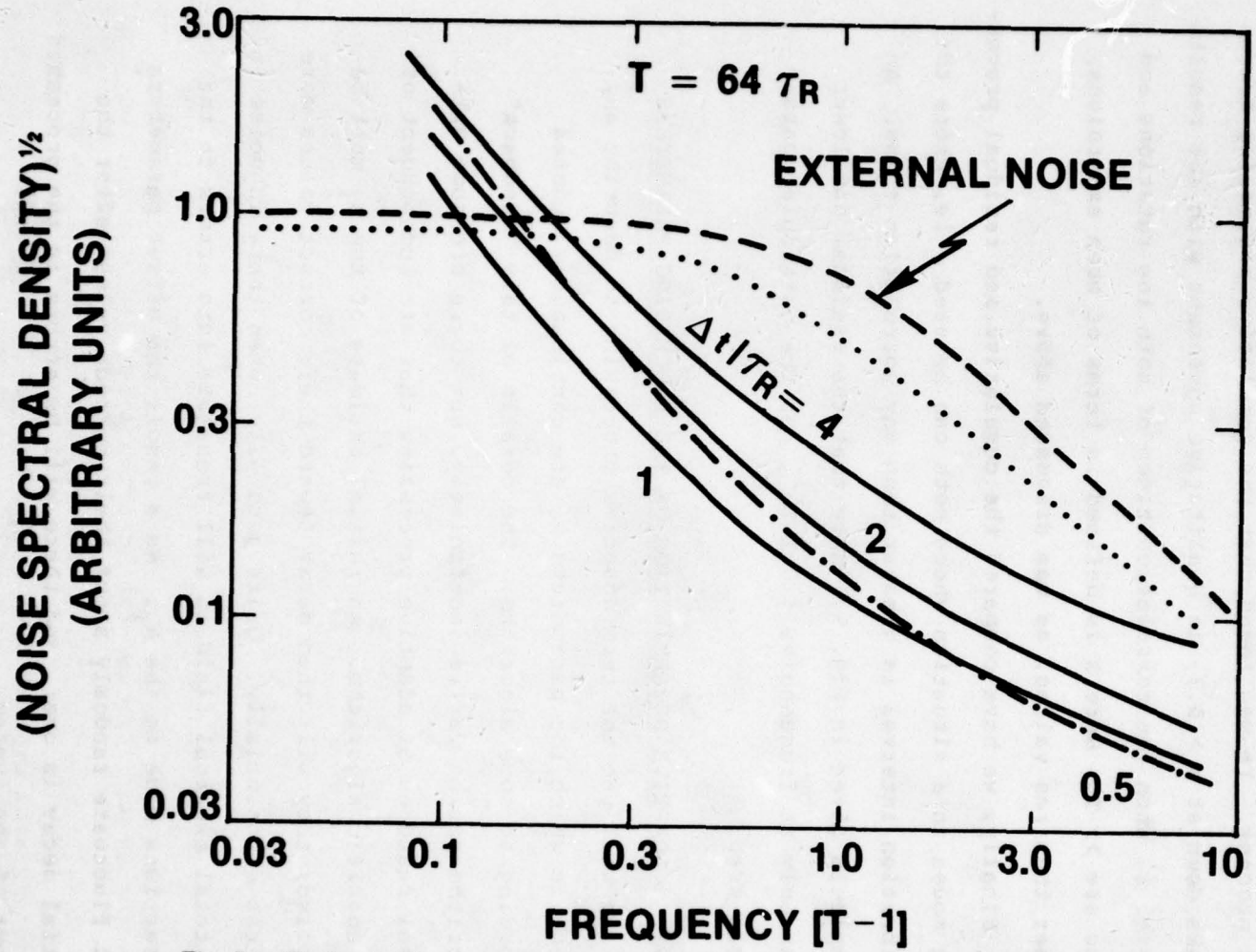

Fig. 5 — Similar to Fig. 3, except that the external noise has a Lorentzian shape, with a correlation time = 0.16T. The dotted line is the result using the residual processing mode, with $\Delta t/\tau_R = 1$.

The general prescription for choosing a feedback algorithm starts with an error function S; we might use, for instance,

$$S = \left(\sum_{i=1}^{4} A_i V_i + V^2/2 \right)^2 / A^2. \qquad (24)$$

This is similar to (9b) with two differences:

(1) The terms corresponding to a linear increase in total field (A_5, V_5) have been dropped. These involve an explicit dependence on t, while adaptive processing is meant to operate continuously, independent of the choice of an origin of time. This does not mean that one can ignore the possibility of a constantly increasing total field, but simply that the error function used in the Least Squares Processing is not suitable.

(2) The error function is not an average over a number of samples.

The correction that is applied to the A_i to make them converge toward their correct values is proportional to $-\partial S/\partial A_i$, evaluated at each data sample. From Eq. 24 the corrections δA_i have the form:

$$\delta A_i = - K_1 \left(V_i - A_i \frac{\Delta H}{A} \right) \frac{\Delta H}{A}, \quad i=1,2,3 \qquad (25a)$$

$$\delta A_4 = - K_2 \frac{\Delta H}{A} \qquad (25b)$$

where $$\Delta H = \left(\sum_{i=1}^{4} A_i V_i + V^2/2 \right)/A. \qquad (25c)$$

It can be shown [16] that continuous application of these corrections will cause the A_i to converge to the same values that a least-squares minimization of S would yield. In Refs. 4-6 a

generalization of Eqs. 25 was considered, wherein averages of the RHS were used to determine the corrections δA_i. When the averaging time was too long it was found that the system became susceptible to runaway instabilities. On the other hand there are no obvious arguments against making the averaging time short, and in the present work we have restricted our attention to the case of a correction being made after each sample (n=1, in the notation of Ref. 6).

To estimate the rate at which the offset parameters converge toward their final values, we suppose that one of them, say A_1, deviates by an amount ΔA_1 from its correct value. If the others have the correct value and there is no external noise we have $\Delta H = V_1 \Delta A_1/A$. (We are assuming that ΔH is sufficiently small that the second term on the RHS of (25a) can be neglected. When there is external noise present ΔH is finite even when $\underline{\Delta A} = 0$. In this case neglect of the second term in (25a) is justified only if $x \ll 1$, with x defined in Eq. 11.) Then the correction δA_1 is

$$\delta A_1 = - K_1 \frac{V_1^2}{A^2} \Delta A_1. \tag{26}$$

This equation formally resembles that for an exponential decay of ΔA_1 toward zero, except that the coefficient determining the rate of decay is not constant. An ensemble or statistical average for the decay constant, or acquisition time, can be defined, however:

$$\tau_{acq}/\Delta t = A^2/(K_1 \overline{V_1^2}). \tag{27}$$

where Δt is the sampling interval.

If $\tau_{acq} < \tau_R$, the correlation time of the platform rotations, Eq. 27 is meaningful only in an ensemble sense. If it happens that V_1 is near zero when the processing system is initiated, A_1 will not be corrected at an appreciable rate until V_1 becomes comparable to its rms value. Since this will require of the order of the correlation time τ_R, we can say that τ_R sets a practical lower limit for the convergence rate of $\underline{A}$. In Fig. 6 we show the results of simulations of the algorithm discussed above which confirm these ideas. We plot an average decay constant for the direction of $\underline{A}$ (the reason for considering only the direction is discussed below) as a function of τ_{acq} as defined in Eq. 27. It is apparent that the decay constant is reasonably well fit by $\tau_{acq} + \tau_R$.

When τ_{acq} becomes of the order of just a few sampling intervals, there is a significant probability that the instantaneous factor multiplying ΔA_1 in (26) would exceed unity; in this case the correction applied to A_1 is too large, and in fact could result in a larger $|\Delta A_1|$ than before the iteration. This leads to the possibility of an exponential runaway of one of the A_i from its correct value, as was observed in the present work and also in Refs. 4-6.

A rather serious problem with the adaptive approach follows from the fact that the averages of V_i^2, and consequently the rate of convergence of the A_i, can vary widely among the three SQUID axes. For instance if $\underline{A}$ is approximately in the direction

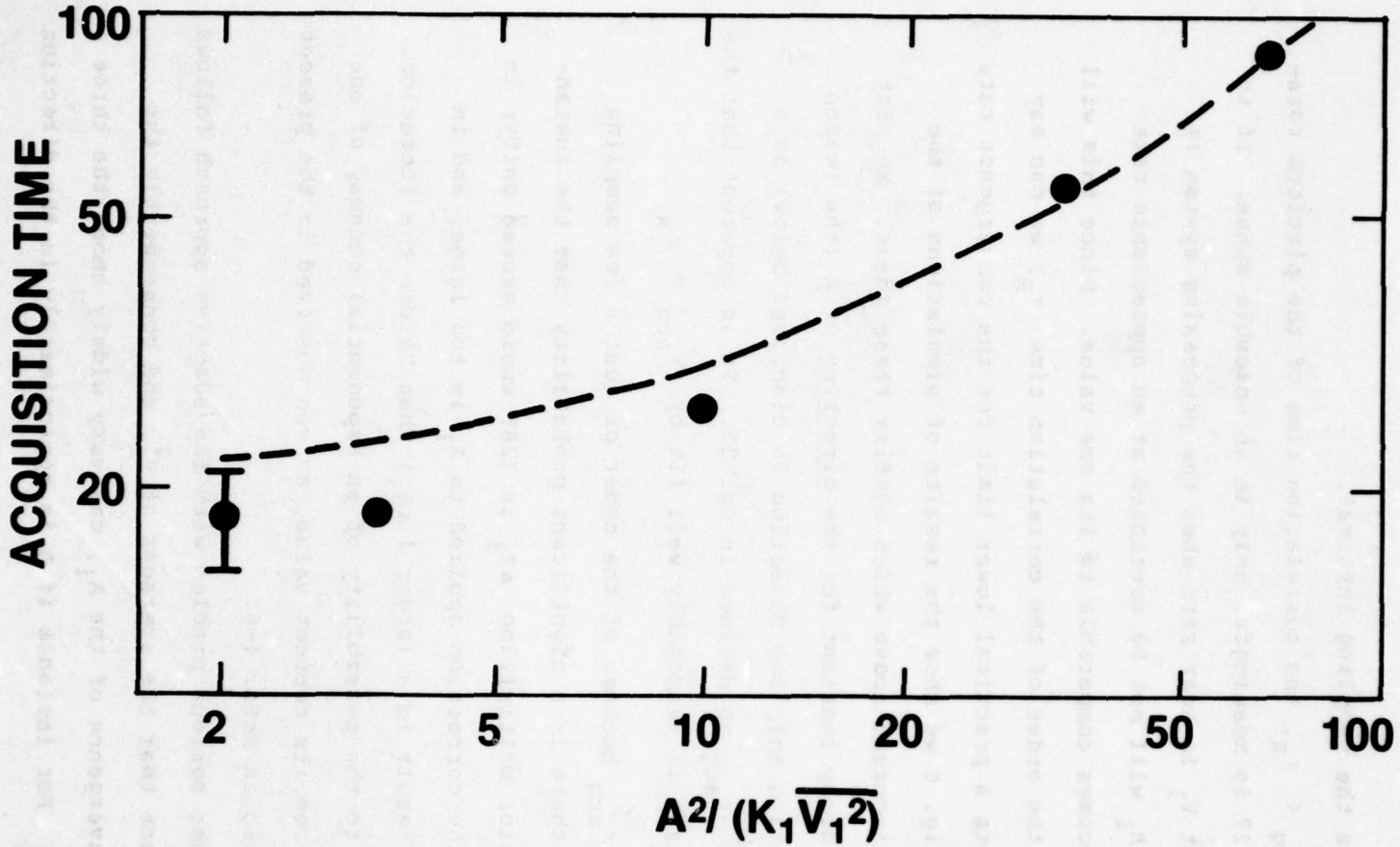

Fig. 6 — A plot of the observed decay time constant of the direction of A toward its correct value, averaged over several trials, as a function of $\tau_{acq} = A^2/(K_1 V_1^2)$. Here V_1 is the SQUID reading along an axis perpendicular to A and K_1 is the corresponding feedback constant, defined in Eq. 25a. The dashed line is $\tau_{acq} + \tau_R$, where τ_R is the correlation time of the rotations which in this case equals 20. All times are in units of Δt, the sampling interval.

of the 3rd axis, we would have $\overline{V_1^2} \cong \overline{V_2^2} \sim \overline{\theta^2}A^2$, and $\overline{V_3^2} \cong 3(\overline{\theta^2})^2A^2$. The rate of convergence of A_3 toward its correct value would be $\sim \overline{\theta^2}$ times slower than for A_1 and A_2, if the same value of K_1 is used for all axes. It might be possible to dynamically adjust K_1 to the rms sensor outputs that are actually present during a run, but this would add considerably to the complexity of the algorithm.

An alternate approach, which was used in most of the simulations in this work, is to suppose that the magnitude of $\underline{A}$ is known with sufficient accuracy that it need not be determined adaptively. From Eq. 4 we find that the error in $\Delta H'$ due to an error ΔA in $|A|$ is

$$H \cong - V^2 \ \delta A/2A^2 \cong - \theta^2 \ \delta A/2. \qquad (28)$$

$|A|$ differs from the earth's field by a factor involving some linear combination of the elements in $\underline{\underline{D}}$. Since the earth's field can be determined to high accuracy with an auxilliary scalar field magnetometer, it is reasonable to assume that A can be known to a part in 10^3. The maximum excursion of θ that was observed for the towed buoy, 10^{-3} rad, would result in an error $5\times10^{-5}\ \gamma$ in the processed output. We can estimate the spectral density of θ^2 in the vicinity of 1Hz, say, by multiplying the in-band noise in θ by the peak excursions of θ. For the towed buoy these numbers have upper limits $\sim 10^{-4}$ rad/ $\sqrt{\text{Hz}}$ and $\sim 10^{-3}$ rad, respectively. If $|A| = 5\times10^4\ \gamma$, we find that a 0.1% error in $|A|$ would lead to a noise contribution $\sim 2\times10^{-5}\ \gamma/\sqrt{\text{Hz}}$.

The remaining term in (4) depends only on the direction of $\underline{A}$, which we denote by the unit vector $\underline{m}$. In most of our simulations of adaptive processing, we used the algorithm

$$\delta m_i = - K V_i \, (\underline{m} \, \underline{V} + V^2/2A), \; i=1,2,3, \tag{29}$$

which is basically the same as (25a), to adjust the direction of $\underline{m}$; during each iteration the magnitude was also adjusted to keep it unity. Note that once $\underline{m}$ is near the correct direction the adjustments (29) have a small effect on its magnitude since $\underline{V}$ is approximately perpendicular to $\underline{m}$. Eq. 29 can be written in terms of components parallel and perpendicular to the direction $\underline{m}$:

$$\delta \underline{m}_\perp = - K V_\perp \Delta H, \tag{30a}$$

$$\delta \underline{m}_\parallel = - K V_\parallel \Delta H, \tag{30b}$$

where

$$\Delta H = \underline{m} \, \underline{V} + V^2/2A. \tag{30c}$$

The part of (29) corresponding to (30b) serves to change the magnitude of $\underline{m}$; such changes are subsequently counteracted by the subsidiary loop which keeps $|\underline{m}|=1$, so that (30b) has no effect. Changes in the direction of $\underline{m}$ are governed by $\underline{V}_\perp$. The acquisition time (for achieving the correct direction) is $\tau_{acq} \cong 2\Delta t/K \, \overline{V_\perp^2})$. Note that this contains no explicit reference to the direction of $\underline{m}$ relative to the coordinate axes. Thus the acquisition time for the direction of $\underline{A}$ is well-defined and independent of the orientation of the coordinate system.

In our simulations we tried passing the adaptively determined $\underline{m}$ through a low-pass filter to remove some of the residual noise, and using this filtered $\underline{m}$ in (30c) to compute the processed output. Table II lists a number of results of these simulations. The time constant τ_{LP} of the low-pass filter, when it was used, was set to be comparable to the acquisition time. The processing noise frequently had a Lorentzian noise spectrum. It can be seen from the Table that there was little relationship between the cutoff frequency of the output noise and that of the input noise. The acquisition time plays a role in adaptive processing somewhat like that of the calibration interval T in the least squares mode. It can be seen that with increasing τ_{acq} the processing noise at low frequencies ($G_{pn}(0)$) is reduced , but not as rapidly as might be expected from the least squares results.

The sequences 1-3, 7-10, and 11-14 correspond to increasing sampling rates, holding all other parameters constant. It is quite surprising, and not understood, that significant improvements in $G_{pn}(0)$ are obtained by increasing the rate even when it is as high as 10 per rotational correlation time (τ_R). In contrast, the least squares processing showed marginal gains once Δt was $< \tau_R$.

All of the results in Table II are for the case of a constant average total field. When a linear rate of change term was added, the processing noise deteriorated seriously. The reason for this can easily be seen by inspection of Eq. 25a or 30a. If ΔH is constantly growing, the corrections to $\underline{A}$ or $\underline{m}$

TABLE II

Summary of simulations of the adaptive processing scheme described in Sec. VI. $G_{pn}(0)$ is the spectral density of the processing noise at low frequencies, and $(2\pi \tau_{pn})^{-1}$ is the cutoff frequency for those cases where $G_{pn}(f)$ had a Lorentzian shape. Where no value for τ_{pn} is given, the shape was significantly different from Lorentzian. τ_R and τ_N are the correlation times for the rotations and external noise, respectively, τ_{acq} and τ_{LP} are described in the text, and Δt is the sampling interval.

#	τ_{acq}/τ_N	τ_{LP}/τ_N	τ_R/τ_N	$\tau_R/\Delta t$	$G_{pn}(0)/G_x(0)$.	τ_{pn}/τ_N
1	0.2	0.2	0.2	5	0.29	-
2	0.2	0.2	0.2	10	0.22	0.13
3	0.2	0.2	0.2	20	0.16	0.10
4	0.2	0	0.2	10	0.35	-
5	5	5	5	10	0.55	2.5
6	5	0	5	10	0.57	1.5
7	0.67	0.60	0.2	2	0.23	-
8	0.67	0.60	0.2	5	0.17	-
9	0.67	0.60	0.2	10	0.145	0.13
10	0.67	0.60	0.2	20	0.145	0.13
11	0.67	0	0.2	2	0.47	-
12	0.67	0	0.2	5	0.29	-
13	0.67	0	0.2	10	0.20	0.15
14	0.67	0	0.2	20	0.15	0.12
15	16.7	0	5	10	0.43	2.4
16	16.7	15	5	10	0.41	3.2

grow correspondingly, and eventually amount to random fluctuations governed primarily by the platform rotations. To construct an adaptive algorithm that will work under these circumstances requires a different error function as a starting point.

An error function that is appropriate to the case of a uniformly increasing field is

$$S = [(\Delta H)_{HP}]^2 = (\underline{A}\,\underline{V}_{HP} + (V^2)_{HP}/2 - A\dot{H}\tau)^2/A^2. \qquad (31)$$

The subscript HP refers to the indicated quantity after having been passed through a high-pass filter of time constant τ. This filtering could be done digitally as part of the processing. The equations for adaptive feedback are the same as Eqs. 25, with the substitutions: $V_i \rightarrow (V_{HP})$; $i = 1,2,3$; $\Delta H \rightarrow (\Delta H)_{HP}$; $A_4 = -A\dot{H}\tau$. Note that the interpretation of A_4 has changed from a measure of the initial offset (which does not appear in $(\Delta H)_{HP}$) to a measure of the rate of change of the total field.

A first iteration of the algorithm suggested above was simulated to demonstrate that the idea is fundamentally sound. A particularly surprising result was that the processing noise is nearly independent of τ - that is, high-frequency information alone seems to be adequate to determine $\underline{A}$ with high accuracy.

Although the adaptive approach probably can be modified to perform as well as the least squares algorithm, the complexity appears to escalate rapidly in assuring convergence of all parameters in a reasonable time, adequate performance in a changing total field, etc. For example, another point that

needs to be considered is the fact that the direction as well as the magnitude of the earth's field will change with time. This means that $\underline{V}$ will have an average offset that grows continuously. While this is not fundamentally objectionable, (assuming the flux-counting/interpolation scheme is used), limitations in the dynamic range of the computer will require that the SQUID outputs ocassionally be reset to zero. Our initial instincts in this study were to favor the adaptive approach, because of its apparent simplicity and ease of implementation. It now appears that the least squares approach is, if anything, simpler to use in practice. Furthermore, the recent rapid advances in microprocessor technology tend to mitigate what at first seemed to be intimidating feature of the latter approach: the simultaneous solution of 5 equations for 5 unknowns. For these reasons the adaptive approach was not pushed further than the point described above.

VII CONCLUSIONS

Most of the work reported here is concerned with theoretical, rather than practical, limits on the success of a TRISCON system. The important conclusions are as follows: The ultimate noise performance of a TRISCON System is set not by the intrinsic sensor noise (if SQUIDs are used) but rather by the magnitude and spectral density of the ambient, geomagnetic noise. The characteristics of the platform motions also enter in, but only via their spectral distribution. In our computer simulations we wished to be able to cover a wide range of conditions that could occur in

practice. This was done by generating ambient noise and platform motions with Lorentzian spectral density. By varying the time constant, or correlation time, the statistics of these quantities could be made to range from uncorrelated (white noise) to a random walk (noise density $\sim f^2$). We have found that a variation of the least squares minimization approach that was termed cumulative processing works well over the entire range of correlation times. The worst case, when both the ambient noise and platform orientation follow a random walk, still resulted in a noise contribution from the processing no greater than the ambient noise. Under less severe conditions the processing noise could be well below the external noise -- i.e. the processed output is an accurate measure of the external total field variations. The processing noise power spectral density (PSD) was found to depend on the acquision time T as $\sim T^{-1}$. (In the simplest implementation of least squares processing, T is the delay between data input and processed output.) Cummulative processing always results in a low-frequency PSD of the processing noise which depends on frequency as f^{-2} or faster. This means that the difference between processed output and the true external field continually grows with random walk statistics. If the external field itself has similar statistics, as seems likely, this drift is not a problem (in the sense that the S/N ratio is the same at all frequencies). If the external fields do not have net drifts, the residual processing approach might be preferable.

The adaptive updating algorithm has an appealing simplicity in

its most straightforward realization. However various practical considerations, such as the existence of a linear increase in the total field due to gradients in the earth's field and the requirement for a well-defined convergence time, tend to escalate the complexity of the processing. In the end it turns out that adaptive processing is at least as complex as a least squares approach.

The dynamic range requirements on the SQUID systems are quite stringent. We have concluded that only a flux-counting/interpolation readout scheme will provide a sufficient digital dynamic range. The use of such a system sets an upper limit on the rotational slew rate of the platform that can be tolerated, rather than on the peak rotational excursions. Unfortunately no candidate platform has been well characterized in this respect. Using a flux counting electronics package that is available commercially, the maximum slew rate would be a few millirad/sec. It appears that this requirement could be satisfied by an underwater towed buoy, but not by an airborne platform. Second-generation SQUID systems may be useable with slew rates 10 or 15 times greater.

The magnitude of the rotational excursions of the platform is important primarily in that it determines whether non-orthogality terms need to be included in the processing. With a currently available triaxial SQUID system (orthogonality within 2×10^{-4} rad) these terms need not be included if the platform is a towed buoy, but must be kept if it is an airborne towed bird.

If it is assumed that a platform, meeting the above requirements under operational conditions, can be found, the following questions about the SQUID hardware remain to be answered:

(1) We do not know whether the settling time/slew rate specifications that have been advertised for a commercial flux-counting SQUID system can in fact be achieved under severe environmental conditions.

(2) It may be that magnetization of adjacent construction material can couple into the magnetometer sensors and degrade the overall performance. General considerations lead us to believe that his will be a low-order effect as long as the susceptibility of the support material is linear in the applied field. However hysteresis or non-linear effects, which are by no means uncommon, could be a problem.

(3) There is no guarantee that the linearity of a flux-counting SQUID system is as good as in the feedback mode. Likewise additional problems involving backlash, flux motions, etc. could develop.

VIII RECOMMENDATIONS

The next stage for this project should be to identify some of the practical, as opposed to theoretical, problem areas. Therefore, it is recommended that a set of flux-counting electronics units for use on an existing NRL Triaxial SQUID instrument be purchased. The system could be mounted on a non-magnetic shake table, such as the one in development for the Panama City Group, and the algorithm developed in this work could be used to process the data from the three SQUIDs. The processed output

would then contain several potential contributions:

(1) The actual ambient field fluctuations that were present. To some extent these could be identified if simultaneous recordings of the output of a state-of-the-art He vapor magnetometer were made. Alternatively, a stationary SQUID oriented along the earth's field could be used.

(2) Spurious components due to non-orthogonality of the sensors. The NRL system was shown to be orthogonal to within 2×10^{-4} rad, but as a double check it would probably be wise to program the full algorithm including the non-orthogonality corrections.

(3) Signals generated by the shake table. It should be established that these are small compared to other contributions.

(4) Errors due to SQUID non-linearity. There may be some way of separating these errors from others by selective choice of rotation axes, direction of the earth's field, magnitude of the platform motions, etc. In any case it appears to be exceptionally difficult to test <u>directly</u> for linearity at the required level (better than a part in 10^6).

The computational requirements for an on-line TRISCON system appear to be reasonably manageable - i.e. the processing could probably be handled by an inexpensive mini-computer. The major expense in realization of the on-line mode would be software development. This would best be left to a future phase of the program.

Finally, the possibility of reducing the motions of an airborne platform should be studied further, and existing platforms should be better characterized, particularly as to their maximum slew rates.

References

1. S.A. Wolf, J.R. Davis, and M. Nisenoff, "Superconducting Extremely Low Frequency (ELF) Magnetic Field Sensors for Submarine Communications," IEEE Trans. Comm. COM-22, 549-554 (1974).
2. S.A. Wolf, M. Nisenoff, and J.R. Davis, "Superconducting ELF Magnetic Field Sensors for Submarine Communications," NRL Report 7720, May 1974.
3. J.R. Davis, R.J. Dinger, and J. Goldstein, "Development of a Superconducting ELF Receiving Antenna," IEEE Trans. AP-25 (2), 223-231 (Nov. 1977).
4. R.J. Dinger and J.R. Davis, "Adaptive Methods for Motion-Noise Compensation in Extremely Low Frequency Submarine Receiving Antennas," Proc. IEEE 64(10), 1504-1511 (1976).
5. R.J. Dinger, J.R. Davis, J.A. Goldstein, and W.D. Meyers, "SQUID ELF Receiving Antenna for Submarine Applications: Final Report," NRL Report 8118, May 1977.
6. R.J. Dinger and J. Goldstein, "Motion Stability Measurements of a Submarine-Towed ELF Receiving Platform," IEEE J. Oceanic Eng. OE-1, (1976).
7. C.H. Sinex, "A Signal Processing Method for Superconducting Total Field Magnetometers," Johns Hopkins University Applied Physics Laboratory Report POR-3168, August 1977.
8. C.H. Sinex, APL memorandum DM-3823/PSA-77-038, Dec. 1977.
9. R. Gasser, W. Payton, E. Greeley, "Instrumented Towed Vehicle Flight Test Report," Naval Air Systems Command Report No. NADC-77238-20, May 1977.

10. B.M. Jones, Memorandum to B.F. Savage "Antenna Stabilization Report" (Naval Surface Weapons Center) dated Aug. 27, 1975.

11. R.L. Forgacs and A. Warnick, "Digital-Analog Magnetometer Utilizing a Superconducting Sensor ," Rev. Sci. Instr. 38, 214 (1967.

12. Private conversations with representatives of SHE Corp. They find empirically that the feedback is stable as long as the total rms instrinsic SQUID noise within the response bandwidth is less than ~ 0.03 flux quanta. This scales as (SQUID noise/$\sqrt{Hz}$) $\sqrt{f_m}$, so a reduction in SQUID noise permits a larger f_m.

13. J.E. Evans and A.S. Griffiths, "Design of a Sanguine Noise Processor Based on World-Wide Extremely Low Frequency (ELF) Recordings," IEEE Trans. Comm. COM-22 528-539 (1974).

14. M.B. Kraichman, "Handbook of Electromagnetic Propagation in Conducting Media," Naval Material Command, 1970 (AD714004).

15. P.W. Hamming, "Numerical Methods for Scientists and Engineers," McGraw-Hill Book Co., NY, 1973.

16. B. Widrow, P.E. Mantey, L.J.Griffiths, and B.B. Goode, "Adaptive Antenna Systems," Proc. IEEE 55, 2143-2158 (1967).

17. L.D. Enochson and R.K. Otmes, "Programming and Analysis for Digital Time Series Data," The Shock and Vibration Center, Naval Research Laboratory, Washington, DC (1968).

Appendix A. EFFECTS OF NON-ORTHOGONALITY TERMS

Here we estimate the error in the value of $\underline{A}$ determined by the least squares method when the non-orthogonality and lack of gain uniformity of the sensors are ignored. Suppose instead that $\underline{\underline{D}}$ is explicitly known. The analysis of Sec. III can be recapitulated, leading to versions of Eqs. 10 that are only slightly modified: (10d) is replaced by:

$$B_i' = -\overline{V_i[\underline{I} + \underline{\underline{D}})V]^2}/2, \qquad \text{(A1)}$$

and all the other equations remain the same. The value of $\underline{A}$ that solves these equations (subsequently referred to as $\underline{A}'$) is the correct value (in the limit of long averaging times). To lowest order in $\underline{\underline{D}}$, we have

$$\underline{\Delta A} = \underline{A}' - \underline{A} = \underline{\underline{M}}^{-1}(\underline{B}'-\underline{B}) \cong -\underline{\underline{M}}^{-1}\,\overline{\underline{V}(\underline{V}\underline{\underline{D}}\underline{V})}, \qquad \text{(A2)}$$

where $\underline{\Delta A}$ is the error in $\underline{A}$ that results from ignoring the error terms. To estimate $\underline{\Delta A}$, we drop the initial offset and rate terms in Eqs. 10 (i=4,5), and transform Eq. (A2) into a reference frame where $A_1' = A_2' = 0$. The equation remains formally the same, except that $\underline{\underline{D}}$ is replaced by its transformed value, $\underline{\underline{D}}'$. Note that the elements of $\underline{\underline{D}}'$ have the same order of magnitude as those of $\underline{\underline{D}}$. The following approximations are then valid if $\underline{\underline{D}}$ is not too large and the platform rotates equally about all axes:

$$\overline{V_1^2} = \overline{V_2^2} = V_o^2$$

$$V_3 = -(V_2^2 + V_2^2)/2H_o$$

$$\overline{V_3^2} = 2V_o^4/H_o^2$$

$$\overline{V_1V_2} = \overline{V_1V_3} = \overline{V_2V_3} = 0 \qquad \text{(A3)}$$

$$\overline{V_1^3} = \overline{V_2^3} = \overline{V_1V_2^2} = \overline{V_1V_3^2} = \overline{V_1^2V_2} = \overline{V_2V_3^2} = \overline{V_1V_2V_3} = 0$$

$$\overline{V_1^2V_3} = \overline{V_2^2V_3} = -2V_o^4/H_o$$

$$\overline{V_3^3} \sim (V_o^6/H_o^3) = \text{negligible}$$

We then have that $\underline{M}$ (along with $\underline{M}^{-1}$) is diagonal, with

$$M_{11} = M_{22} = V_o^2$$

$$M_{33} = 2V_o^4/H_o^2.$$

Likewise $(\underline{B}' - \underline{B}) = \underline{\Delta B}$ takes on a simple form:

$$\Delta B_1 = 2(D'_{13} + D'_{31})V_o^4/H_o$$

$$\Delta B_2 = 2(D'_{23} + D'_{32})V_o^4/H_o$$

$$\Delta B_3 = 2(D'_{11} + D'_{22})V_o^4$$

The effect of an error in $\underline{A}$ on the computed $\Delta H'$ (Eq. 4) naturally divides into two components:

(1) An error in the magnitude contributes via the second (quadratic) term: $\delta H_1 = -(V^2/2|A|^2)\,\Delta|A|$ (A4)

We have $\Delta|A| = \Delta A_3 = \Delta B_3/M_{33}$, so

$$\delta H_1 = -(D'_{11} + D'_{22})V^2/2H_o \qquad \text{(A5)}$$

Note that this is comparable to the error term (Eq. 5) that explicitly follows from ignoring $\underline{\underline{D}}$ in Eq. 3.

(2) The error in $\Delta H'$ resulting from an error in the direction of $\underline{A}$ is given by $\delta H_2 \cong (V_1 \Delta A_1 + V_2 \Delta A_2)/H_o$. (A6)
The rms value of this error is

$$\delta H_2)_{rms} \cong 2V_o^3(D'_{13}+D'_{31}+D'_{23}+D'_{32})/H_o^2. \qquad \text{(A7)}$$

This is down from previous error terms by a factor $\cong V_o/H_o << 1$, so need not be considered.

Appendix B. APPLICABILITY OF LINEARIZED LEAST SQUARES SOLUTION

In this section the criterion for using a linearized approximation of Eqs. 10 for the Least Squares solution is estimated. We note that the solution to the full set of equations satisfies $\underline{\underline{M}}'\underline{A} = \underline{B}$, where $M'_{ii} = M_{ii} - S$ for i = 1,2,3, and the other elements of $\underline{\underline{M}}'$ are the same as those of $\underline{\underline{M}}$. The linear approximation amounts to setting $\underline{\underline{M}}' = \underline{\underline{M}}$. We can guess that in order for this approximation to be valid it should not change the determinant of $\underline{\underline{M}}$ by more than a fractional amount x. The determinant is most conveniently evaluated in a reference frame where $A_1 = A_2 = 0$. (We have the freedom of using any coordinate frame we wish , since it can be shown that a coordinate transformation amounts to an orthogonal transformation of $\underline{\underline{M}}$, which in turn leaves $|\underline{\underline{M}}|$ unchanged.) Using the results in (A2) for the elements of $\underline{\underline{M}}$, we find:

$$|\underline{\underline{M}}| \cong 2V_o^8 \overline{t^2}/H_o^2$$

$$|M'| \cong (V_o^2-S)^2 \, (2V_o^4/H_o^2-S)\overline{t^2}. \qquad \text{(B1)}$$

$$|M'|/|M| \cong (1-S/V_o^2)^2 \, (1-SH_o^2/2V_o^4).$$

The dominant dependence on S is in the last term, so we propose

$$x = SH_o^2/V_o^4 \cong \overline{H_x^2}/(H_o^2(\overline{\theta^2})^2). \qquad \text{(B2)}$$

Here we have used that $V_o/H_o \cong \theta_{rms}$, and also that S is approximately (but <u>not</u> exactly) $\overline{H_x^2}$. Note that the parameter plotted in Fig. 1 is actually the fourth root of x as defined above.

Appendix C. DETAILS OF THE COMPUTER SIMULATIONS

The purpose of this section is to provide some information about the details of the computer simulations described in the text. To do this, we will provide a line-by-line exegesis of one of the Fortran programs that was used extensively. The one chosen was designed to apply the least squares algorithm with cumulative processing. Many of the routines used to test other algorithms differed only in relatively minor details. This program is descended from previous iterations, and has a few vestigial elements that are harmless, but serve no function.

line 1 Load time parameters: NLOOP = number of times the main loop is to be repeated. This was chosen large enough to yield adequate signal/noise in overall output. NPT = number of samples within each loop, usually set at 4096. NCAL is the number of samples to be used in each calibration interval. NAVE, NPLT are defined in conjunction with the PSD routine.

lines 2,3 Specific to the local system

line 5 These variables were made double precision to be on the safe side. It probably isn't necessary.

line 8 These variables relate to the statistics of the external noise and platform rotations.

line 18, etc. This call fills the array DTHETA with a set of random numbers which have a normal (gaussian) distribution, and an rms value ANGRMS. Line 13 is an initializing call for the routines.

lines 22-25 These perform the digital equivalent of passing the uncorrelated numbers in DTHETA, etc. (white noise) through a low-pass filter. The resulting array of correlated numbers has a PSD $G(f) = 2\,(ANGRMS)^2\,\Delta t/[1+(2\pi f\,\Delta t\,TAUROT)^2]$, where Δt is the sampling interval and (TAUROT Δt) is the correlation time of the platform rotations. In the case of VN the new array replaces the original one. For the angle variables the correlated terms are intermediate steps in determining sensor outputs.

lines 26-32 Here the SQUID outputs are calculated, assuming that initially the earth's field points in the direction of the third axis. It is assumed that there is a rotation ϕ about the first axis, and then a rotation θ about the (new) second axis. This results in the following components of the earth's field:
$H_1 = H\sin\phi$, $H_2 = -H\sin\theta\cos\phi$, $H_3 = H\cos\theta\cos\phi$.
An external noise component (VN) is added only to the third axis, since components in the other directions are indistinguishable (to first order) from rotations. Note that our choice of the initial direction of $\underline{H}$ permits small-angle approximations to be used for sin and cos, resulting in significant savings in computer time. There is no loss of generality in this choice, since the algorithm that is being tested involves vector equations. Consequently the results cannot

depend on the choice of coordinate axes. In general there will also be rotations about the third axis; the displacements so generated can always be duplicated by some combination of θ and ϕ.

lines 34-47 The matrix $\underline{\underline{M}}$ and vector $\underline{B}$ (here called A) defined in Eqs. 10c and 10d are accumulated within each calibration interval. The interval runs from INIT to INIT+NCAL.

line 48 This call inverts the set of equations characterized by $\underline{\underline{M}}$ and $\underline{A}$ and puts the roots in the array A.

lines 49-53 Here the square of the deviations of the calculated A_i from their true values are accumulated. Actually the errors in direction(DN) and inverse magnitude (DXNORM) of $\underline{A}$ are computed, since they are simply related to the expected errors in processed output - c.f. Eqs. 14 and 15.

line 56 Here we calculate the processed output over the range of the calibration interval. It is equivalent to Eq. 18, except that we have subtracted away the true change in total field. The latter is all contained in the continuation line. The result is the processing error, and is stored in the array VN. In line 58 we accumulate the square of the processing noise. For this particular algorithm the mean square processing error is unbounded, so there is real point in doing this.

lines 60-65 The quantity $H_p(0)$ in Eq. 18, here called XHO, is calculated for use in the next calibration interval.

lines 68-83 After the entire array VN has been filled with processing error values, we divide it in two parts and take the Fourier transform of both. (Thanks to a property of the complex Fourier transform, this can be done with a single FFT call.) The real and imaginary parts of the two transforms are appropriately squared and averaged, and stored in the array S. To further smooth the PSD, NAVE adjacent terms in S are co-added and stored in Y. The k'th element of Y corresponds to a frequency $(2k-1)NAVE/(NPT\ \Delta t)$. The variance of the points in Y can be further reduced by setting NLOOP > 1. For a more detailed discussion of PSD calculations, see Ref. 17.

lines 85-end The averages of various quantities are computed and output. The contents of Y (appropriately scaled) are output on the printer as a funtion of index (freqency) in the form of a log-log plot using the facility-supplied routine ONPLOT. The accuracy with which the points are plotted is not very great, but the statistical significance of each point is even less. Since Y(1) includes the total drift in the processed output, it was usually many orders of magnitude greater than subsequent points. It was therefore discarded (by setting Y(1)=Y(2)).

```
                SOURCE LISTING              ASC FAST FORTRAN COMPILER       RELEASE FTF:

CSN               STATEMENT                 CP OPTIONS = (A)                        DATE


0001              PROGRAM LEAST(NLOOP,NPT,NCAL,NAVE,NPLT)
0002              CALL R$STOP
0003              COMMON/FFTDAT/Q(4096)
0004              REAL F(NPLT),Y(NPLT),X(NPT),S(NPT)
0005              REAL*8 M(5,5),A(5),ST(25),D,VD(5,NCAL),VSQ(NCAL)
0006              REAL  H,HC,V(3,NPT),DTHETA(NPT),DPHI(NPT),VN(NPT)
0007              DATA DRATE,DXNORM,DN,DH0SQ,DHSQ1,DHSQ2,H0/6*0.0,5.0E4/
0008              READ(5,101) TAUROT,TAUM,ANGRMS,VNRMS,RATE
0009        101   FORMAT(10X,F15.5)
0010              Y=0.
0011              C1=1./(1.+TAUROT)
0012              C2=1./(1.+TAUM)
0013              CALL SETVRN(0)
0014              DO 150 NS=1,NLOOP
0015              THETA=ANGRMS/SQRT(1.+2.*TAUROT)
0016              PHI=THETA
0017              VNOLD=VNRMS/SQRT(1.+2.*TAUM)
0018              CALL VRNORM(DTHETA,NPT,0.,ANGRMS)
0019              CALL VRNORM(DPHI,  NPT,0.,ANGRMS)
0020              CALL VRNORM(VN,    NPT,0.,VNRMS)
0021              DO 10 I=1,NPT
0022              THETA=C1*(TAUROT*THETA+DTHETA(I))
0023              PHI  =C1*(TAUROT*PHI  +DPHI(I))
0024              VN(I)=C2*(TAUM*VNOLD+VN(I))
0025              VNOLD=VN(I)
0026              H=H0+RATE*I
0027              P=PHI**2
0028              T=THETA**2
0029              V(1,I)=4*PHI*(1.-P/6.)
0030              V(2,I)=-H*THETA*(1.-T/6.)*(1.-P/2.)
0031              V(3,I)=RATE*I+VN(I)-H*(P+T)/2.
0032        10    CONTINUE
0033              DO 80 INIT=1,NPT,NCAL
0034              M=0.
0035              A=0.
0036              DO 50 K=1,NCAL
0037              DO 20 J=1,3
0038        20    VD(J,K)=V(J,INIT+K-1)-V(J,INIT)
0039              VD(4,K)=1.
0040              VD(5,K)=FLOAT(K)
0041              DO 30 I=1,5
0042              DO 30 J=1,5
0043        30    M(I,J)=M(I,J)+VD(I,K)*VD(J,K)
0044              VSQ(K)=(VD(1,K)**2+VD(2,K)**2+VD(3,K)**2)/2.
0045              DO 40 J=1,5
0046        40    A(J)=A(J)-VSQ(K)*VD(J,K)
0047        50    CONTINUE
0048              CALL DSIMEC(M,A,5,1,D,ST)
0049              XNORM=1./DSQRT(A(1)**2+A(2)**2+A(3)**2)
0050              DXNORM=DXNORM+(XNORM-1./(H0+RATE*INIT))**2
```

```
EAST            SOURCE LISTING              ASC FAST FORTRAN COMPILER       RELEASE FTF)

   CSN            STATEMENT                   CP OPTIONS = (A)                        DATE

   0051           DN=DN+(XNORM*A(1)-V(1,INIT)/H0)**2+(XNORM*A(2)-V(2,INIT)/H0)**2
   0052           DRATE=DRATE+(RATE+A(5)*XNORM)**2
   0053           DH0SQ=DH0SQ+(A(4)*XNORM-VN(INIT))**2
   0054           IF(INIT.EQ.1) XH0=A(4)*XNORM
   0055           DO 70 K=1,NCAL
   0056           DH=XH0+XNORM*(A(1)*VD(1,K)+A(2)*VD(2,K)+A(3)*VD(3,K)+VSQ(K))
                 1   -RATE*(INIT+K-1)-VN(INIT+K-1)
   0057           VN(INIT+K-1)=DH
   0058           DHSQ1=DHSQ1+DH**2
   0059     70    CONTINUE
   0060           IF(INIT+NCAL.GT.NPT) GOTO 80
   0061           X1=0.
   0062           DO 75 J=1,3
   0063           V1=V(J,INIT+NCAL)-V(J,INIT)
   0064     75    X1=X1+V1*(A(J)+V1/2.)
   0065           XH0=XH0+X1*XNORM
   0066     80    CONTINUE
   0067     201   FORMAT(4X,'NPT',9X,'NCAL',8X,'TAUROT',6X,'TAUNOISE',5X,
                 1   'VNRMS',7X,'ANGRMS',6X,// 1X,2I12,1P4E12.3////
                 2  4X,'RATE',8X,'MSD RATE',5X,'MSD N',7X,'MSD XNORM',3X,
                 3   'MS OFFSET',3X,'MS ERROR(1)',1X,'MS ERROR(2)',//
                 4   1X,1P9E12.3)
   0068           M1=NPT/2
   0069           DO 110 I=1,M1
   0070           X(2*I-1)=VN(I)
   0071     110   X(2*I)=VN(I+M1)
   0072           NLOG=IFIX(ALOG10(FLOAT(NPT))/ALOG10(2.)-.9)
   0073           CALL FOURIN(-1,M1)
   0074           CALL FOURTR(X,X,VN,M1,NLOG)
   0075           NMAX=NPT/4
   0076           S(1)=2.*(X(1)**2+X(2)**2)
   0077           DO 120 I=2,NMAX
   0078           K=2*I
   0079           S(I)=(X(K)**2+X(K-1)**2+X(NPT-K+4)**2+X(NPT-K+3)**2)
   0080     120   CONTINUE
   0081           DO 130 I=1,NPLT
   0082           DO 130  J=1,NAVE
   0083     130   Y(I)=Y(I)+S(NAVE*(I-1)+J)
   0084     150   CONTINUE
   0085           DO 160 I=1,NPLT
   0086           F(I)=ALOG10(FLOAT(I))
   0087     160   Y(I)=ALOG10(Y(I)/(NAVE*NPT*NLOOP))
   0088           DHSQ2=Y(1)
   0089           Y(1)=Y(2)
   0090           NTOT=NPT*NLOOP/NCAL
   0091           DN=DN/NTOT
   0092           DXNORM=DXNORM/NTOT
   0093           DH0SQ=DH0SQ/NTOT
   0094           DHSQ1=DHSQ1/NTOT
   0095           DRATE=DRATE/NTOT

   0096           PRINT 201,NPT,NCAL,TAUROT,TAUM,VNRMS,ANGRMS,RATE,DRATE,
                 1      DN,DXNORM,DH0SQ,DHSQ1,DHSQ2
   0097           CALL SNPLOT(F,Y,NPLT)
   0098           STOP
   0099           END
```